In vitro investigations of the metabolism of Victoria pure blue bo dye to identify main metabolites for food control in fish

1.1 Contexte

L'objectif de l'étude *in vitro* du projet Metacolor était d'explorer plus largement le métabolisme des TAMs, en conservant comme modèles VPBO et MG, afin de déterminer si l'approche méthodologique permettait d'imputer un ou plusieurs métabolites pertinents *in vitro* au métabolisme de la truite. Une équipe spécialisée en éco-toxicologie et compétente sur la préparation de fractions microsomales chez le poisson, le FFPW en République Tchèque, a été contactée. J'ai pu ainsi me former dans leur laboratoire sur la méthodologie de préparation des fractions subcellulaires et sur leur incubation. Plusieurs types de fractions subcellulaires (microsomes, fractions S9 de truite) ont pu être ramenées dans notre laboratoire, dont certaines induites par la β-naphtoflavone, un inducteur du CYP1A, afin de poursuivre les expérimentations.

1.2 Méthodologie et principaux résultats

Méthodologie de mise au point des conditions d'incubation

Les fractions sub-cellulaires ont été préparées par une technique de centrifugation différentielle (microsomes, S9) extraites de chaque truite. Les premières incubations tests réalisées au FFPW, avec des temps d'incubation de 30 min, ont été injectées pour analyse par LC-HRMS à mon retour au laboratoire et n'ont pas permis de détecter une formation de métabolites du MG ou du VPBO. Il a alors été nécessaire d'optimiser ces conditions. Profitant d'une méthode développée au laboratoire pour un projet de toxicologie, nous avons optimisé les conditions de température et durée d'incubation pour aboutir à la détection des métabolites.

Des substrats spécifiques des principales activités du CYP450 ont été utilisés: la phénacetine pour le CYP1A2, le diclofénac pour le CYP2C9, la méphénytoine pour le CYP2C19, le midazolam pour le CYP3A4, le bupropion pour le CYP2B6, et la chlorzoxazone pour le CYP2E1. Les métabolites associés ont été détectés et quantifiés, en faisant varier les temps d'incubation et les températures.

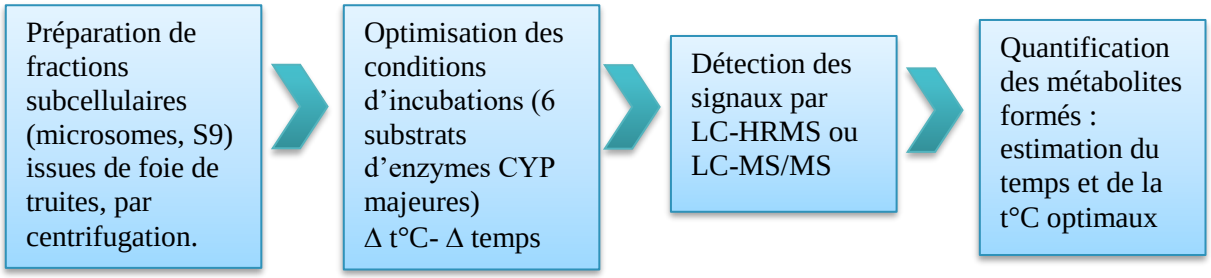

Méthodologie de recherche des métabolites formés :

En utilisant les conditions optimales (2 h à 20 °C), nous avons incubé MG et VPBO avec les fractions microsomales de truite et les fractions S9 induites avec la β-naphtoflavone puis analysé le surnageant dans un système LC-LTQ-Orbitrap-HRMS. Les co-facteurs appropriés ont été ajouté pour initier les réactions de phase I ou de phase II.

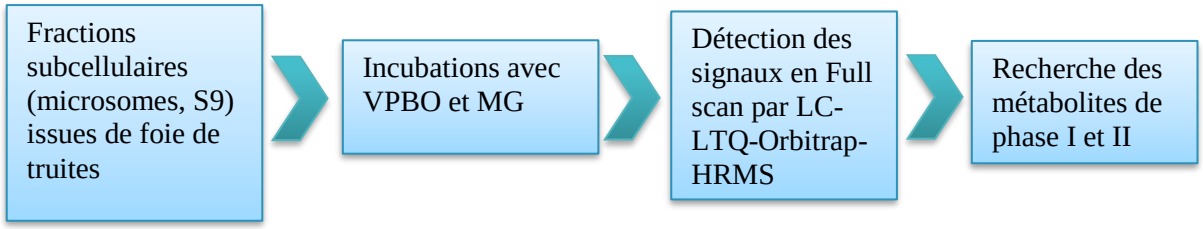

Principaux résultats :

Objectifs : appréhender les techniques de préparation microsomales, d'incubation. Rechercher les métabolites du VPBO formés *in vitro*, comparer le métabolisme à celui du MG, identifier un métabolite majeur

Mise au point des conditions d'incubation

-Observation d'une activité pour: CYP1A, CYP2-like et CYP3A-like, suite à la formation d'acétaminophène, OH-diclofénac, OH-midazolam
-Activité optimale pour 2h d'incubation et 20°C

Recherche des métabolites formés

-Optimisation d'une méthode générique de détection LC-HRMS
-Détection de 16 métabolites du VPBO formés par réactions de phase I, résultant en particulier de réactions avec le CYP1A.
-Aucun métabolite de phase II détecté.
-Le principal métabolite détecté, le dééthyl-VPBO, a été fragmenté par CID afin de déterminer sa structure chimique.

1.3 Conclusion

Cette étude a permis d'appréhender les différents types de fractions microsomales de poisson, depuis leur préparation jusqu'à leur utilisation pour initier une étude de métabolisme. L'objectif était d'obtenir des résultats de première approche *in vitro* pour l'étude du métabolisme du VPBO. Ces résultats suggèrent que la biotransformation de VPBO dans le foie de poisson est médiée par les enzymes CYP formant à la fois des métabolites désalkylés et des métabolites N-oxydés ainsi qu'une réduction de la double liaison conduisant à une leuco-forme, le dééthyl-leuco-VPBO. Le métabolite N-dééthylé de VPBO est celui retrouvé en plus forte intensité. MG suit une voie similaire *in vitro* pour la déalkylation, mais pas pour les métabolites N-oxydés. Cette étude est probante afin d'obtenir rapidement un aperçu du ou des métabolites majeurs pouvant être intéressants à confirmer lors d'une étude *in vivo* de persistance, afin de définir un ou des résidus marqueurs. Le dééthyl-VPBO a été retrouvé le plus intense, cependant le mécanisme de réduction de la double liaison a été peu détecté *in vitro*, alors que les leuco formes sont connues *in vivo* comme majeures pour MG et CV. Il nous est alors apparu nécessaire de proposer une expérimentation *in vivo* pour appréhender la pharmacocinétique du VPBO, ce qui a été l'objet du 3^{e} article.

Chemosphere 238 (2020) 124538

Contents lists available at ScienceDirect

Chemosphere

journal homepage: www.elsevier.com/locate/chemosphere

In vitro investigations of the metabolism of Victoria pure blue BO dye to identify main metabolites for food control in fish

Estelle Dubreil [a, *], Luc Sczubelek [a], Viktoriia Burkina [b], Vladimir Zlabek [b], Sidika Sakalli [b], Galia Zamaratskaia [c], Dominique Hurtaud-Pessel [a], Eric Verdon [a]

[a] ANSES Fougeres Laboratory, European Union Reference Laboratory for Antibiotic and Dye Residue in Food, CS 40608-Javene, F-35306, Fougeres, France
[b] University of South Bohemia in Ceske Budejovice, Faculty of Fisheries and Protection of Waters Vodnany, South Bohemian Research Center of Aquaculture and Biodiversity of Hydrocenoses, Zatisi 728/II, 389 25, Vodnany, Czech Republic
[c] Swedish University of Agricultural Sciences, Department of Molecular Science, P.O. Box 7015, SE-750 07, Uppsala, Sweden

HIGHLIGHTS

- The *in vitro* metabolism of Victoria pure blue BO (VPBO) dye was investigated.
- HRMS analysis shows that VPBO is metabolised into 16 metabolites.
- The CYP1 isoform is involved in VPBO metabolism.
- Deethyl-VPBO metabolite holds promise as a biomarker of exposure to VPBO in rainbow trout.

GRAPHICAL ABSTRACT

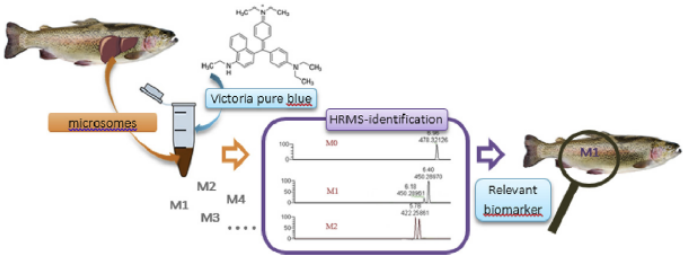

ARTICLE INFO

Article history:
Received 22 May 2019
Received in revised form
25 July 2019
Accepted 7 August 2019
Available online 10 August 2019

Handling Editor: Jim Lazorchak

Keywords:
Dyes
Aquaculture
Chemical residues
LC-HRMS
Microsomes
Cytochromes P450

ABSTRACT

Although banned, dyes, such as Victoria pure blue BO (VPBO), are illicitly used in aquaculture to treat or prevent infections due to their therapeutic activities. The present study examined the formation of phase I and phase II metabolites derived from VPBO using trout liver microsomes and S9 proteins. The well-known malachite green (MG) dye was also studied as a positive control and to compare its metabolism with that of VPBO. First, we optimised the incubation conditions for the detection of VPBO and MG metabolites by studying the formation of cytochrome P450 (CYP) substrates. Using the determined conditions (2 h at 20 °C), we incubated VPBO with trout microsomal and S9 fractions induced with β-naphtoflavone, and analysed the supernatant in a LC-LTQ-Orbitrap-HRMS system. The *in vitro* assays led to the detection of 16 VPBO metabolites from Phase I reactions, arising in particular from reactions with CYP1A. No metabolites were detected from Phase II reactions. The main metabolite detected, deethyl-VPBO, was CID-fragmented to determine its chemical structure, and thus recommend a potential biomarker for the control of VPBO in farmed fish foodstuffs.

* Corresponding author.
E-mail address: estelle.dubreil@anses.fr (E. Dubreil).

https://doi.org/10.1016/j.chemosphere.2019.124538
0045-6535/

1. Introduction

Over the past 40 years, the aquaculture industry has grown exponentially in response to the increase in the world population, but also in response to consumer demand for fish-based foods and new food trends. Therefore, the maintenance of healthy fish-farming conditions is needed to minimise the risk of disease, reduce fish stress and minimise the environmental impact (Burka et al., 1997). Pharmacologically active substances such as antibiotics, pesticides or dyes are often used in fish farming. In the past, some triarylmethane dyes, such as malachite green (MG) and crystal violet (CV), were employed to prevent fungal infections and as antibacterial and antiparasitic agents. MG has been administered as prophylactic agent for both fish and fish oocytes for over 60 years (Foster and Woodbury, 1936). However, due their toxicity for human consumption (Schneider et al., 2004; Srivastava et al., 2004) and harmful effects on animals, dyes were subsequently banned and MG is in particular strictly regulated in the EU and the US, applying a policy of zero tolerance (WHO/FAO, 2015) with a detection capability required at 2 and 1 $\mu g\,kg^{-1}$ respectively. Although MG has been banned, it can still be detected in fish products imported from Asian countries (Gräslund and Bengtsson, 2001; Hashimoto et al., 2011; Tao et al., 2011; Fallah and Barani, 2014). MG, CV as well as brilliant green and their reduced (colourless) leuco-forms are currently targeted by analytical methods such as tandem mass spectrometry (MS/MS) to detect and quantify their residues in aquaculture foodstuffs (Andersen et al., 2015, 2018; Schneider and Andersen, 2015). Today, a new dye from the triarylmethane family, Victoria pure blue BO (VPBO), is suspected of use by the aquaculture industry in lieu of MG and CV (Tarbin et al., 2008; Reyns et al., 2014). For example, VPBO contamination was once reported by the European rapid Alert System for Food and Feed (RASFF-portal, European Commission) for fish imported from Vietnam (notification 2010.1372). In a recent report from the European Food Safety Authority (EFSA), VPBO was classified among the dyes for which a reference point for action (RPA) could be established in the near future, because it was assigned a toxicological screening value (TSV) of 0.0025 $\mu g\,kg^{-1}$ body weight per day (Penninks et al., 2017), due to its (potential) genotoxicity. Thus, there is a need to study the fate of dyes in fish tissues, including those of the triarylmethane-family compounds, as well as any possible toxic metabolites that have not been described so far.

For first intention metabolism studies on a chemical substance, *in vitro* experiments using sub-cellular fractions often deliver a snapshot of the potential metabolites that can help to understand the xenobiotic metabolism before carrying out *in vivo* studies. Xenobiotic metabolism reactions are categorised into Phase I and Phase II reactions. Phase I metabolism of numerous xenobiotics and endogenously produced compounds, including drugs and environmental pollutants can be studied using the cytochrome P450 (CYP) enzyme system, frequently responsible for Phase I oxidative metabolism. Phase II comprises conjugation or synthetic reactions (e.g., methylation, glucuronidation, sulfation), which generally lead to the increased solubility of xenobiotics (Guengerich, 1992). Thus, investigation of Phase I and II metabolic reactions is important in terms of fish health and welfare. *In vitro* incubations with sub-cellular fractions from fish are the first ecotoxicological approach to determine whether and how the xenobiotic is metabolised by Phase I enzymes (Vestergren et al., 2012; Ren et al., 2014; Zlabek et al., 2016) or Phase II enzymes or a combination of both (James et al., 2008; Shen et al., 2012; Ikenaka et al., 2013).

In vitro systems for determining main metabolites of pharmacologically active dyes were rarely employed. However, few experiments were conducted for MG incubation with microbial cultures (Singh et al., 1994; Cha et al., 2001) and for crystal violet (Bumpus and Brock, 1988). These studies released a first set of data about triarylmethanes metabolism complementary to the implementation of *in vivo* fish or mammalian studies (Plakas et al., 1996; Doerge et al., 1998; Culp et al., 1999b).

The aim of this study was to identify metabolites of VPBO and MG formed during Phase I and Phase II metabolism. To do so, we first determined the best incubation conditions for Phase I reactions to detect VPBO and MG metabolites. The potential metabolites of VPBO were identified by molecular separation and detection with liquid chromatography-high resolution mass spectrometry (LC-HRMS) and by data mining using MetWorks® software. Finally, we proposed a chemical structure for the main metabolite detected.

2. Materials and methods

2.1. Chemicals and reagents

2.1.1. Metabolite investigations

MG oxalate salt (product number 46396), VPBO (product number 76773) and an internal standard (IS) for MG (MG-d_5) (product number 33945) were purchased from Sigma-Aldrich (St. Quentin-Fallavier, France). The IS for VPBO (CV-d_6) (product number OP045) was purchased from Witega (Berlin, Germany). Stock solutions of MG and VPBO (1 mM) were prepared in 100% methanol (MeOH). Stock solutions were further diluted from 200 µM to 10 µM to obtain several concentrations ranging from 1000 nM to 50 nM. ISs were prepared at 70 nM for MG-d_5 and 30 nM for CV-d_6 in methanol. The cofactors dihydronicotinamide-adenine dinucleotide phosphate (NADPH), uridine 5′-diphosphoglucuronic acid (UDPGA), 3′-phosphoadenosine-5′-phosphosulfate (PAPS), L-glutathione reduced (GSH), S-adenosylmethionine (SAM) and alamethicin were purchased from Sigma-Aldrich. The positive controls for Phase II reactions were obtained from Chemservice (West Chester, PA, USA) for 7-hydroxycoumarin, and Sigma-Aldrich for apigenin and acetaminophen.

Acetonitrile (ACN), MeOH, ammonium acetate and formic acid were of HPLC grade. Water was purified using a Milli-Q system (Millipore, city, MA, USA).

2.1.2. Analysis of CYP activities

Phenacetin, diclofenac, bupropion, midazolam, acetaminophen, mephenytoin, chlorzoxazone, 4′-OH-diclofenac, 1′-OH-midazolam, OH-bupropion, OH-mephenytoin, 6-OH-chlorzoxazone, diclofenac-d_4 (IS), acetaminophen-d_4 (IS) were purchased from Sigma-Aldrich. The stock solutions of CYP substrates were prepared in DMSO and stored at −20 °C. The stock solutions of metabolites were prepared in MeOH and stored at −20 °C.

2.2. Fish

Rainbow trout of both sexes (n = 16) with length 30 ± 2.0 cm (mean ± standard deviation) and weight 373 ± 63 g, were purchased from a local commercial hatchery (Vodnany, Czech Republic). Fish were handled according to national and institutional guidelines for the protection of human and animal welfare. The fish were acclimated for 14 days and fed with commercial fish food (BioMar, Denmark) at 1% of body weight per day. To avoid effect of dietary bioactive compounds, fish were not fed last 24 h of acclimatization period. Additionally, β-naphtaflavone (BNF) was administered to four fish at 50 $mg\,kg^{-1}$ for 48 h. Fish were sacrificed according to the ethical rules of the EU-harmonised Animal Welfare Act of the Czech Republic. The unit is licensed (No. 53100/2013-MZE-17214) according to the Czech National Directive (Act No 246/1992 on the protection of animals against cruelty). Before

sampling fish hepatic tissues, fish were anesthetised in an ice bath and their spinal cords were cut immediately thereafter. Hepatic tissues were collected and stored at −80 °C before the extraction of microsomes and S9.

2.3. Preparation of microsomes and S9 fractions

Microsomal and S9 fractions were prepared from each individual fish by using the differential centrifugation method in two (for microsomes) or one (for S9) step(s) as described previously (Burkina et al., 2013). The prepared S9 fractions were only recovered from induced BNF fish whereas microsomal fractions were only recovered from non-treated fish by BNF.

Protein levels in prepared fractions were estimated spectrophotometrically using the method described in (Smith et al., 1985) with bovine serum albumin as a standard. Microsomes were suspended in buffer and stored at −80 °C. The microsomes were diluted in phosphate potassium buffer to a protein content of 10 mg mL^{-1} prior to use.

2.4. Measurement of CYP activity over time and temperature

Trout microsomes or S9 fractions were incubated with a cocktail of specific CYP substrates based on the methodology of Anthérieu et al. (2010). Some specific human substrates were used to evaluate CYP activity: phenacetin for CYP1A2, diclofenac for CYP2C9, mephenytoin for CYP2C19, midazolam for CYP3A4, bupropion for CYP2B6 and chlorzoxazone for CYP2E1. In the first experiment for enzymatic assessment over time, the cocktail of substrates was incubated for different times (30 min, 1 h, 2 h or 3 h) at 25 °C. Briefly, reaction mixtures (0.1 mL) contained 2 mg of microsomal or S9 proteins in an incubation medium of 50 mM phosphate potassium buffer (pH 7.4) and cofactor NADPH (1 mM). In the second experiment for enzymatic assessment over temperature, the cocktail of substrates was incubated for 2 h at different temperatures (12 °C, 17 °C, 21 °C, 25 °C, 37 °C). The reaction mixture was the same as described above. Once the set time had elapsed, the reaction was stopped by the addition of 100 µL ice-cold MeOH to prevent further metabolite formation and spiked with ISs (diclofenac-d_4 and acetaminophen-d_4) at 5 µM. Then, the supernatant was vortex-mixed and centrifuged at 10,000×*g* for 10 min. The clear supernatant was analysed using LC-LTQ-Orbitrap-HRMS for quantification of CYP activity by measuring metabolite formation: acetaminophen for the substrate phenacetin, 4′-OH-diclofenac for the substrate diclofenac, 4-OH-mephenytoin for the substrate mephenytoin, OH-midazolam for the substrate midazolam, OH-bupropion for the substrate bupropion and 6-OH-chlorzoxazone for the substrate chlorzoxazone.

These metabolite solutions were diluted in MeOH and phosphate buffer (50%/50%, v/v) to obtain freshly prepared mixture calibration standards including the ISs diclofenac-d_4 and acetaminophen-d_4.

2.5. In vitro identification of MG and VPBO metabolites

2.5.1. Identification of phase I metabolites

All assays were processed on ice and in the dark, because triarylmethanes are light-sensitive.

The incubation mixture contained, in the following order: the appropriate volume of phosphate buffer to obtain a final total volume of 100 µL, 2 mg mL^{-1} microsomal fraction or 1.42 mg mL^{-1} induced S9 fraction, substrate at 1 µM (VPBO or MG) and 1 mM NADPH to initiate the reaction. The incubation mixture was vortexed and incubated for 2 h at 20 °C. After 2 h, the reaction was stopped by the addition of 100 µL ice-cold MeOH spiked with the CV-d_6 IS at 10 µg $L^{-1}$and the mixture was vortexed and centrifuged at 10,000×*g* for 10 min. The supernatant was analysed using an LC-LTQ-Orbitrap-HRMS. Calibration standards were prepared between 50 nM and 1 µM with addition of the substrate (VPBO or MG positive control) after the end of the 2 h incubation.

Several negative controls with no substrate or with no microsomes or S9 protein fractions were also prepared to confirm the absence of interfering compounds and to identify any non-metabolically formed compounds. These three control incubations were necessary to confirm the quality of the process: (1) the “inactive microsomes” control is an incubation mix in which microsomes were pre-incubated at 60 °C for 45 min to inactivate them; (2)- the “blank” control is an assay without substrate (VPBO or MG) or cofactor (NADPH) added; (3) the “without cofactor” control is an assay to check that the enzymatic reaction is inactive. In addition, the MG substrate was used as positive control for Phase I investigations and also to compare Phase I metabolism of MG and VPBO.

2.5.2. Identification of phase II metabolites

The incubation mixture contained, in the following order: the appropriate volume of phosphate buffer to obtain final total volume of 100 µL, 1.42 mg mL^{-1} S9 fraction, alamethicin at 25 µg mL^{-1} on ice for 15 min for pre-incubation if UDPGA was included, substrate at 1 µM (VPBO or MG or positive control), mix composed of cofactors NADPH, GSHred, UDPGA, PAPS, SAM (1 mM, 5 mM, 2 mM, 0.1 mM, 0.1 mM respectively) or cofactors tested separately: GSHred to test the gluthatione-S-transferase reaction, UDPGA to test the UDP-glucuronyl-S-transferase, PAPS to test the sulfotransferase reaction, SAM to the test methyltransferase reaction. The incubation mixture was vortexed. After 3 h, the reaction was stopped by the addition of 100 µL ice-cold MeOH spiked with the CV-d_6 IS at 10 µg L^{-1}. When the reaction was completed, the mixture was vortexed and centrifuged at 10,000×*g* for 10 min. The supernatant was analysed using LC-LTQ-Orbitrap-HRMS.

For quality control, blank incubations without substrate and control samples without S9 proteins were also prepared. Positive controls were added at 50 µM for each of the four following reactions: 7-hydroxycoumarine was tested as substrate for glucuronidation, apigenine for sulfation, acetaminophen for glutathione conjugation and epinephrine for methylation.

2.6. Analysis instrument settings

2.6.1. Metabolite profile analysis

The decrease in the parent compound concentrations and the formation of metabolites were both measured. Metabolites were identified using the metabolite identification software MetWorks® 1.3.0. SP1. Software (Thermo Fisher Scientific, Waltham, MA, USA). The analyses were conducted on the Thermo Fisher Accela LC system coupled to an LTQ-Orbitrap XL mass spectrometer (Thermo Fisher, Bremen, Germany). The reversed-phase LC separation was performed on a Phenomenex Luna C18 (2) column (Torrance, CA, USA) (150 × 2.0 mm, 3 µm) at 25 °C. Elution was performed by means of a gradient of ammonium acetate (10 mM) with 0.1% of formic acid (mobile phase A) and 100% acetonitrile (mobile phase B) at a flow rate of 0.2 mL/min. The gradient conditions were as follows: from 0 to 4 min, ramp up linearly from 98 to 2% of mobile phase A and hold for 8 min, then ramp back over 1 min to initial conditions and hold for 5 min to re-equilibrate the system. The injection volume was 10 µL. The mass spectrometer was operated with an electrospray ionisation probe in positive mode using the following source parameters: sheath gas flow rate of 30 arb; auxiliary gas flow rate of 10 arb; sweep gas flow rate of 2 arb; ion spray voltage of 5 kV; capillary temperature of 275 °C; capillary

voltage of 35 V; and tube lens of 90 V. The instrument was calibrated using the manufacturer's calibration solution, consisting of three mass calibrators (i.e., caffeine, tetrapeptide MRFA and Ultramark) to reach mass accuracies in the 1−3 ppm range. The instrument was operated in full-scan mode from *m/z* 100−1000 at a resolving power of 60,000 (full width at half maximum), allowing detection of VPBO and MG as their MG^+ or $VPBO^+$ positive ions, as well as detection of metabolite formation using MetWorks. Exact masses of the peaks detected by this software were extracted with a mass window of 5 ppm around the ionised precursor ion to confirm or reject their identity. The MG and VPBO recoveries were calculated as follows: $R = (ci \times 100)/c0$, where ci is the measured concentration of sample i, and c0 is the initial concentration. For confirmation of the identity of the major metabolite (deethylleuco), MS^2 exact mass fragmentation of the compound was performed in the LTQ-Orbitrap mass analyser. The energy for collision-induced dissociation (CID) was set at 35 eV, with an isolation width of *m/z* 1.

2.6.2. CYP activity assay

LC analysis was carried out on the same instrument as for metabolite investigation. However, the chromatographic separation was performed on a reversed phase HPLC column Agilent Zorbax RX-C8 (2.1 mm, 150 mm, 5 µm) equipped with a guard column Agilent C8 (12.5 mm, 2,1 mm, 5 µm). Chromatographic separation was carried out using two mobile phase preparations consisting of mobile phase (A) water with 0.1% formic acid, and mobile phase (B) pure analytical grade acetonitrile with 0.1% formic acid. The gradient conditions were as follows: from 0 to 6 min, ramp linearly from 98 to 10% of mobile phase A, then ramp over 0.1 min to initial conditions and hold for 6 min to re-equilibrate the system. The flow rate was set at 0.25 mL/min, the injection volume was 20 µL and the column oven was maintained at 25 °C. The mass spectrometer was operated with an electrospray ionisation probe in positive mode using the following source parameters: sheath gas flow rate of 55 arb; auxiliary gas flow rate of 10 arb; sweep gas flow rate of 2 arb; ion spray voltage of 4.5 kV; capillary temperature of 350 °C; capillary voltage of 35 V and tube lens of 90 V. The instrument was operated in full-scan mode from *m/z* 50−800 at a resolving power of 60,000 (full width at half maximum). The accurate mass of metabolites were theoretically calculated for their $[M + H]^+$ species and monitored at *m/z* 152.0706 for acetaminophen, *m/z* 256.10999 for OH-bupropion, *m/z* 235.1077 for 4-OH-mephenytoin, *m/z* 185.9952 for 6-OH-chlorzoxazone, *m/z* 342.0804 for OH-midazolam, *m/z* 312.0189 for 4′-OH-diclofenac, *m/z* 156.0957 for acetaminophen-d_4, *m/z* 300.0491 for diclofenac-d_4, with a mass tolerance of 5 ppm for quantification purposes.

3. Results and discussion

Here, we studied the *in vitro* biotransformation of VPBO and compared it with MG to identify potential metabolite biomarkers for this dye and structurally similar dyes. These biomarkers will be useful for developing a control strategy in view of establishing future RPAs for non-allowed pharmacologically active substances present in food of animal origin (EFSA CONTAM Panel et al., 2018).

3.1. Optimisation of mass spectrometry and liquid chromatography conditions

In this study, an analytical method was developed to detect VPBO and MG and their metabolites. First, for the mobile phase (pump A), a mixture of 10 mM L^{-1} ammonium acetate and 0.1% formic acid was selected. The pH of the mobile phase was adjusted to 3.5. For MG, whose pKa is 6.9, ionisation reaches 100% (Alderman, 1985). This mobile phase has already been tested in a previous study (Dubreil et al., 2019). The triarylmethane dyes or derivative-types are molecules with an apolar tendency (log P (MG) = 0.062 and estimated log P (VPBO) = 3.48 from Chemspider). Triarylmethanes and their metabolites (leucobases) are commonly eluted by using reversed-phases. We tested three hard-core shell columns (Phenomenex Kinetex C18 2.6 µm, Phenomenex Luna C18 3 µm, Agilent Zorbax-XDB-C8 5 µm), and the Luna column was ultimately chosen for its better response, larger number of points per peak, and also for its generation of slightly longer retention times for the parent compounds (MG and VPBO), which make it able to detect more polar metabolites with lower retention times. A gradient starting from 98% of aqueous mobile phase A and up to 98% of organic mobile phase B was selected for a satisfactory elution of the maximum amount of polar metabolites. In addition to chromatographic optimisation, HRMS conditions on an LTQ-Orbitrap system were optimised for the detection of dyes. Source electrospray conditions, such as capillary voltage, tube lens temperature and curtain gas were adjusted for the two parent compounds, i.e. MG and VPBO. Given that these parent compounds are naturally positively charged, detection was operated only in positive mode.

3.2. CYP activity

For the first time, a sensitive LC-HRMS approach was used to quantify the six CYP model-substrate metabolites in the incubation cocktail.

In the cocktail, the enzymes monitored correspond to CYP1A2, CYP2C9, CYP2C19, CYP3A4, CYP2B6 and CYP2E1, which were included because they are all major enzymes involved in mammalian metabolism (Lewis, 2004) and some are also expressed in fish. Fish CYP enzymes have begun to be studied more recently, particularly to understand the effects of aquatic pollution on various species, zebrafish being a particularly studied species. In fish, the most studied enzymes are CYP1A and CYP3A-like (Jönsson et al., 2010; Burkina et al., 2018). Trout may metabolise some mammalian substrates using the same enzymes as mammalian or via different CYPs (Connors et al., 2013).

Given that preliminary incubations (not described) in trout microsomes did not lead to the production of metabolites, we measured CYP activities to determine the best conditions for their production. The measures were carried out in basal enzyme activity conditions for microsomes that were not induced. To do so, we used a quantification method based on detection by MS that was developed earlier in the laboratory for a study on human cells (Ferron et al., 2016).

Among the six CYPs measured, we observed activity for three of them: CYP1A, CYP2-like, and CYP3A-like, following the formation of acetaminophen, OH-diclofenac, OH-midazolam, respectively (Fig. 1). The metabolite OH-bupropion, probably metabolised by CYP2-like in fish, was detectable, but the MS signal was too weak to be quantified. The quantification of metabolites shows that for CYP1A and CYP3A-like, maximum metabolite production was reached after 3 h of incubation with 700 and 1300 pmol of metabolites per mg of protein, i.e. 3.8 and 7.2 pmol min^{-1} mg^{-1} protein, respectively. However, the formation of OH-diclofenac, probably ensured by the CYP2-like enzyme also, was best detected after 2 h of incubation at a rate of 1000 pmol of metabolites per mg of protein, i.e. 8.3 pmol min^{-1} mg^{-1} of protein. The OH-diclofenac production rate decreased only after 2 h of incubation (see Fig. 1). An overall incubation time of 2 h was thus chosen for the study of dye metabolism, to observe the formation of potential (MG and VPBO) metabolites of interest and to avoid reaching a maximum concentration of product that would prevent any comparison

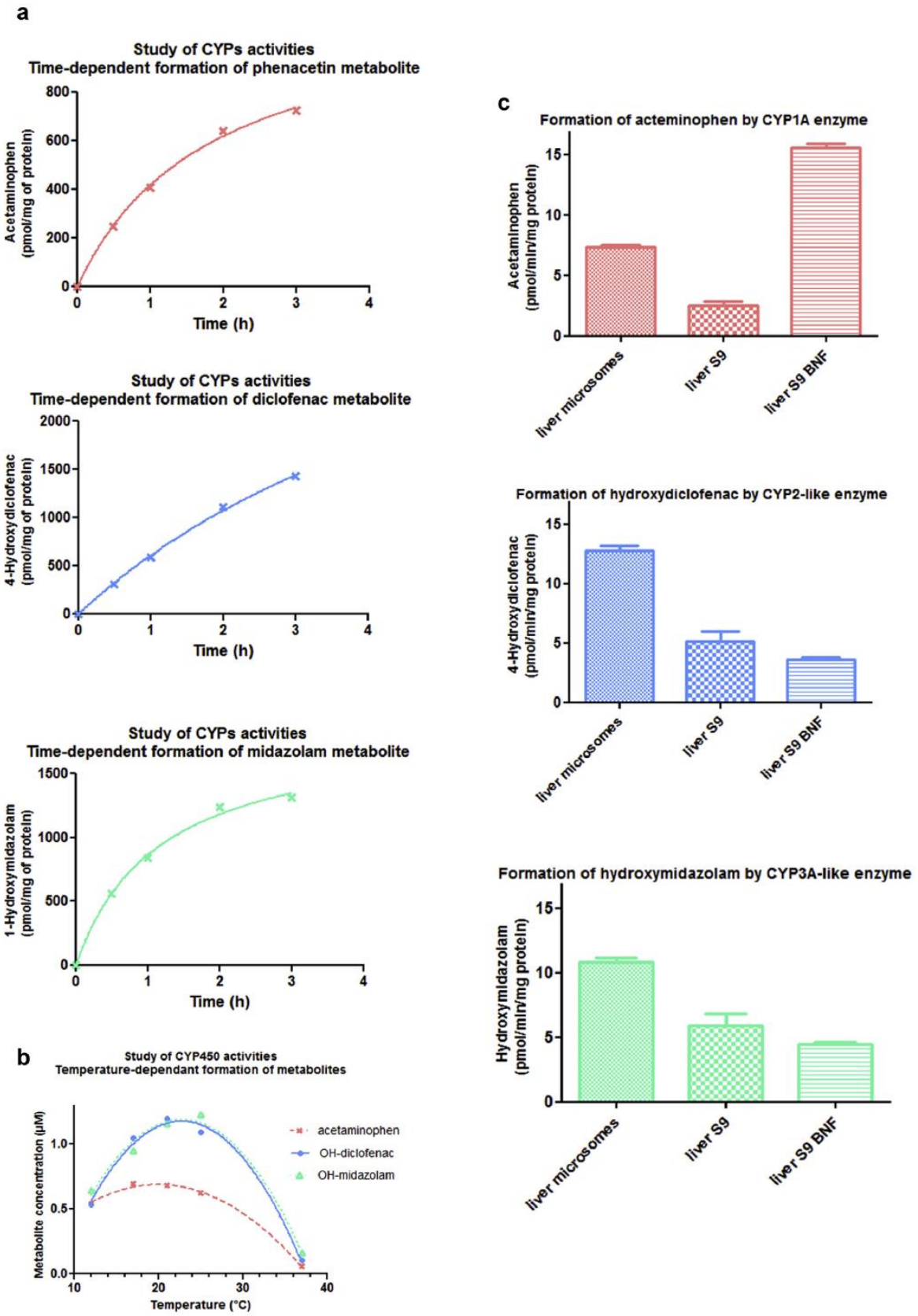

Fig. 1. Study of CYP activity by metabolites formation analysis for method optimisation. Fig. 1a Non induced microsomes at 2 mg mL^{-1}: [S] = 100 µM; [NADPH] = 1 mM; T° = 25 °C; pH7,4. Fig. 1b Non induced microsomes at 2 mg mL^{-1}: [S] = 100 µM; [NADPH] = 1 mM; Time = 2 h; pH7,4. Fig. 1c Metabolites concentration markers of CYPs activities in different liver subfractions.

between the tests. Once the optimal incubation time had been defined, the temperature conditions were studied. In the literature, the temperatures for incubation in trout enzymatic media range from 12 to 25 °C (Connors et al., 2013; Zlabek et al., 2016). Connors et al. (2013) performed the assays at the physiologically realistic temperature of 11 °C to describe the baseline activity of rainbow trout to biotransform selected pharmaceuticals to which it is environmentally exposed, without any specific enzyme inducer. Naab et al. (Nabb et al., 2006) also reported that trout NADPH-CYP reductase is reduced at temperatures lower than the optimal temperature of 25 °C. In our study, the optimal temperature for rainbow trout was between 20 and 25 °C, because we observed a high rate of production of acetaminophen, OH-diclofenac and OH-midazolam. These optimal conditions for CYP catalytic reactions were set up for further detection of VPBO and MG metabolite formation.

3.3. Phase I metabolism of VPBO

In fish, *in vitro* metabolism studies of xenobiotics using microsomal fractions are still relatively rare. As mentioned above, this study was not only conducted to obtain ecotoxicological data, but also to help develop a food control strategy with regard to dyes and to counteract any attempt of misuse of triarylmethanes or structurally related chemical substances. These new toxico-chemical data on dye metabolism may also be useful for increasing the knowledge on the fate of dyes in the environment and their bioaccumulation in fish following illegal treatments in aquaculture or following rejections from dye factories. For such Phase I metabolism studies, microsomal or S9 liver fractions, in contrast to cell cultures have the great advantage of being simple to purchase and to use, and are also easy to preserve. They can be readily employed to investigate the effects induced by chemical contaminants of emerging concern on aquatic organisms; especially for effects that will depend mostly on the biotransformation of the contaminant. Biotransformation generally leads to the formation of more polar metabolites, which can often be eliminated more rapidly than the parent compound (Holčapek et al., 2008). Thus, *in vitro* studies simulate the capacities and mechanisms of transformation of these metabolic products by the liver (Smith et al., 2012; Sakalli et al., 2018). The microsomes contain mostly CYP membrane-bound elements and may be preferable to S9 fractions for the studies of Phase I metabolism. S9 fractions, containing both cytosolic and microsomal enzymes, are generally more diluted and thus considered less active. Zhang et al. (2017) reported that it is necessary to use a larger amount of S9 protein than for microsomes, often five times, to achieve the same level of activity under similar incubation conditions.

3.3.1. Conditions for metabolite detection

Experiments were conducted on two sub-cellular fractions: microsomes and S9 fractions. Additionally, S9 fractions from fish previously injected with BNF (inducer of CYP1A) were used in the present study (Lněničková et al., 2018). Results were acquired for both sub-cellular fractions, giving more information on the effect of CYP1A, by comparing the intensities of the peaks of different metabolites in microsomes and S9 fractions induced with BNF (Table 1).

Detection and identification of *in vitro* metabolites were based on the presence of their protonated molecules $[M+H]^+$ or directly charged M^+ as for the VPBO parent molecule (Villar-Pulido et al., 2011).

First, blank controls were examined to ensure the validity of the results. Heating the liver fraction enzymes to 60 °C or incubating enzymes in the absence of NADPH did not produce any metabolites nor did it produce a decrease in the parent compound VPBO. This result suggests that VPBO is sensitive to Phase I enzymatic transformations in the presence of a metabolic biotransformation cofactor, and that no key factor other than an enzymatic reaction is needed to induce metabolism. In addition, recovery of 65% was obtained for VPBO in induced S9 fractions, suggesting that 35% of VPBO was metabolised following incubation, whereas 50% of MG was metabolised (Table 2). In addition, the recovery was assessed at 30% for VPBO in microsomes (supplementary data, not assessed for MG), almost the same results compared to S9 fractions. No metabolites were detected in incubations without cofactor. Blank samples without cofactor NADPH also confirmed that samples were not contaminated.

3.3.2. Phase I metabolites and comparison with MG metabolism

Several types of phase I metabolic reactions were identified during the incubation of VPBO, either with trout microsomes or S9 fractions. The different biotransformations are listed in Table 1 together with their associated molecular formulae, mass error between measured and calculated mass, retention times and intensity of the peaks obtained in the microsome or S9 incubation environments. The extracted ion chromatograms of proposed metabolites are shown in Fig. 2.

3.3.2.1. Deethylation series. The incubation of VPBO with trout microsomes resulted in the formation of successive deethylation. All metabolites M1 to M5 were detected in positive mode due to the presence of an amino group in their structure already positively charged. Polarities of the deethyl metabolites increased with the number of deethylations, such that retention time was the shortest for the quintuple N-deethyl-VPBO (M5). The first intense peak was observed for the N-deethylation reaction (M1: *m/z* 450.2903), with an intensity in count per second (cps) three times higher in the S9 incubation medium than in the microsome incubation medium. This result suggests that deethyl-VPBO is not a chemical transformation product, but that the metabolic reaction is carried out at least partly by CYPs. The single deethylation led to isomers (see §3.5) with a difference in intensity between their respective peaks. Further deethylations up to the quintuple deethyl-VPBO (M2-M3-M4-M5) were detected and monitored in the incubation medium with the intensity of the respective recorded peaks logically decreasing as the number of deethylations increased. A metabolite corresponding to a single demethylation, with a relatively weak peak, was also observed as a dealkylation reaction (M6: *m/z* 464.3053) as well as a deethyl-demethyl metabolite (M7: *m/z* 436.2746).

Proposed structures for metabolites are shown in Fig. 3 representing the putative metabolic pathway for VPBO. The same sequential dealkylation was first described by Culp et al. (1999a), in an *in vivo* study in rodents. That study predicted the oxidative MG pathway by the sequential N-demethylation of the dye to yield mono-, di-, tri-, and tetra-demethyl derivatives. In our experiments, MG was used as positive control for Phase I reactions. We assumed that Phase I reactions for MG following *in vitro* incubation would be successful in light of the study by Cha et al. (2001) in which a microsomal fraction of *C. elegans* was cultured with MG, and indicated that CYP is involved in the production of N-demethylated derivatives. In our trout microsomal or S9 incubations, up to three demethylations were successfully monitored (Supplementary Table 1) – as reported by Cha et al. (2001) although a tetra-demethyl-MG has also been observed *in vivo* (Culp et al., 1999a).

3.3.2.2. Oxidation series. The N-oxidation reaction of VPBO resulted in five derivatives eluted at 6.0 and 6.2 min for oxidised isomers M8, and then for M9, M10, M11 which are oxidative metabolites

Table 1
In vitro LC-Orbitrap-HRMS data of Victoria pure blue bo and its metabolites in trout.

Compound ID	Reaction	Molecular Formula	Calculated mass	Measured mass	Error (ppm)	RT (min)	Intensity [cps] Microsomes	Intensity [cps] Induced S9
M0	VPBO	**$C_{33}H_{40}N_3$**	**478.3216**	478.3215	0.2	6.9	189198482	316747654
M1	N-deethylation	$C_{31}H_{36}N_3$	450.2903	450.2898	1.1	6.3	21942897	70692673
				450.2899	0.9	6.1		13086030
M2	double N-deethylation	$C_{29}H_{32}N_3$	422.2590	422.2586	0.9	5.9	28852160	22453456
				422.2585	1.2	5.8		24176979
M3	triple N-deethylation	$C_{27}H_{28}N_3$	394.2277	394.2274	0.8	5.4	6716069	9538127
				394.2274	0.8	5.3		821764
M4	quadruple N-deethylation	$C_{25}H_{24}N_3$	366.1964	366.1961	0.8	5.0	642681	1050160
M5	quintuple N-deethylation	$C_{23}H_{20}N_3$	338.1651	338.1648	0.9	4.7	49310	392221
M6	N-demethylation	$C_{32}H_{38}N_3$	464.3059	464.3053	1.3	6.7	530412	1557917
M7	deethylation + demethylation	$C_{30}H_{34}N_3$	436.2746	436.2742	0.9	6.2	95237	147517
M8	oxidation	$C_{33}H_{40}N_3O$	494.3165	494.3161	0.8	6.2	321539	868052
				494.3161	0.8	6.0		496954
M9	deethylation + oxidation	$C_{31}H_{36}N_3O$	466.2852	466.2847	1.1	5.9	221919	712927
						6.1		198557
M10	double deethylation + oxidation	$C_{29}H_{32}N_3O$	438.2539	438.2537	0.5	5.6	151577	277638
M11	triple deethylation + oxidation	$C_{27}H_{28}N_3O$	410.2226	410.2222	1.0	5.1	41240	192955
M12	oxidation + deshydrogenation	$C_{33}H_{38}N_3O$	492.3008	492.3003	1.0	5.5	82405	360567
M13	deethylation + oxidation + deshydrogenation	$C_{31}H_{34}N_3O$	464.2695	464.2687	1.7	5.2	ND	184850
M14	double deethylation + oxidation + deshydrogenation	$C_{29}H_{30}N_3O$	436.2382	436.2375	1.6	5.9	16113	277094
M15	triple deethylation + oxidation + deshydrogenation	$C_{27}H_{26}N_3O$	408.2069	408.2069	0	5.6	68245	219607
M16	deethylation + double bound reduction	$C_{31}H_{38}N_3$	452.3059	452.3055	0.9	10.2	ND	545914

Table 2
VPBO and MG recoveries after incubation with trout S9 fractions.

Assay	VPBO	MG
Phase I reactions	65 ± 2%	52 ± 2%
Phase I + II reactions	66 ± 1%	ND
Phase II reactions	102 ± 12%	ND
Phase I + II (GSH conjugation)	59 ± 1%	159% [a]
Phase II (GSH conjugation)	97%	ND
Phase I + II (UDPGA conjugation)	40%	67 ± 17%
Phase II (UDPGA conjugation)	89%	ND
Phase I + II (PAPS conjugation)	70%	50%

[a] High recovery achieved due to matrix effect.

that undergo successive deethylations at earlier retention times of 5.9 min, 5.6 and 5.1 min, respectively. For isomers M8 (*m/z* 494.3165), the +16 Da shift can surely be attributed to the oxidation of a nitrogen atom, probably on a N-diethylaniline moiety for the most intense peak at 6.2 min, and on the N-ethylnaphtylamine moiety for the less intense peak at 6.0 min. The M8 isomers also gave more intense peaks in the induced S9 incubation medium compared with the microsome incubation medium. However, the principal isomer M8 was detected once in a blank sample without addition of the NADPH cofactor, specifically in the sample prepared with the S9 fraction. Further, it was not detected in the inactive control sample. This appears to suggest that the oxidation reaction can also occur in some other (bio)chemical conditions if sufficiently oxidative.

The same observation was made for M9 (*m/z* 466.2852), when VPBO undergoes oxidation and deethylation. This metabolite was also observed in a blank sample without addition of the NADPH cofactor. The further double deethylation (M10, *m/z* 438.2539) and triple deethylation (M11, *m/z* 410.2226) associated with oxidation were specifically tracked in microsomes and in S9 incubation media. Another type of reaction was observed: a dehydrogenation reaction associated with oxidation generated a Δ *m/z* +14 compared with VPBO. This mass shift can be attributed to N-hydroxylation following dehydrogenation by formation of a double bond between nitrogen and a methyl group at the end an oxime ($+O\text{-}H_2$) (Holčapek et al., 2008). This reaction may occur preferably on the N-deethylaniline to form metabolite M12 (*m/z* 492.3008). A similar process of deethylation can be applied to M12 to form M13 (*m/z* 464.2695), M14 (*m/z* 436.2375), and M15 (*m/z* 408.2069).

The process of N-oxidation for MG has been described by Doerge et al. (1998). Culp et al. (1999b) also proposed a mechanism for the metabolism of MG and leuco-malachite green that can be oxidised to intermediate compounds that react with DNA to generate liver- and thyroid-DNA adducts. In our *in vitro* study, either with microsomes or S9, none of these oxidised metabolites of MG were detected.

3.3.2.3. Double bond reduction series. The double bond reduction is the first well-known metabolic reaction for triarylmethanes, such as MG or CV. This redox reaction was for instance observed as a biotransformation *in vitro* forming leuco-MG in the fungus *C. elegans* (Cha et al., 2001). The authors also demonstrated the involvement of CYPs in this conversion. The double bond reduction has also been depicted many times in edible fish tissues where the leuco-form may accumulate and persist for several months longer than parent compound (Plakas et al., 1996; Thompson et al., 1999; Turnipseed et al., 2005). We assumed that the same reaction can occur for VPBO on the double bond between the two aryl groups. In addition, this reaction was previously observed in our laboratory during some metabolomics studies in trout (Dubreil et al., 2019). Thus, we reviewed all our chromatograms for peaks corresponding to the leucobase of VPBO of *m/z* 480, as well as the leucobases of the N-deethylated metabolites. First, we observed that VPBO leuco-metabolites were absent from all standard and control samples, whereas the reduced leuco-form of MG can occur in solution and was detected in negative controls (inactivated by temperature and without NADPH) and in standards in solution. In incubation media with S9 fractions, one leuco-metabolite of VPBO was recorded, the metabolite M16 (*m/z* 452.3055) corresponding to the leuco-deethylated VPBO. M16 was only detected in induced S9 media, not with microsomes nor in controls. Therefore, we assume that leuco-VPBO metabolites occur less spontaneously than leuco-MG, which also indicates the prominent role of CYP enzymes for the

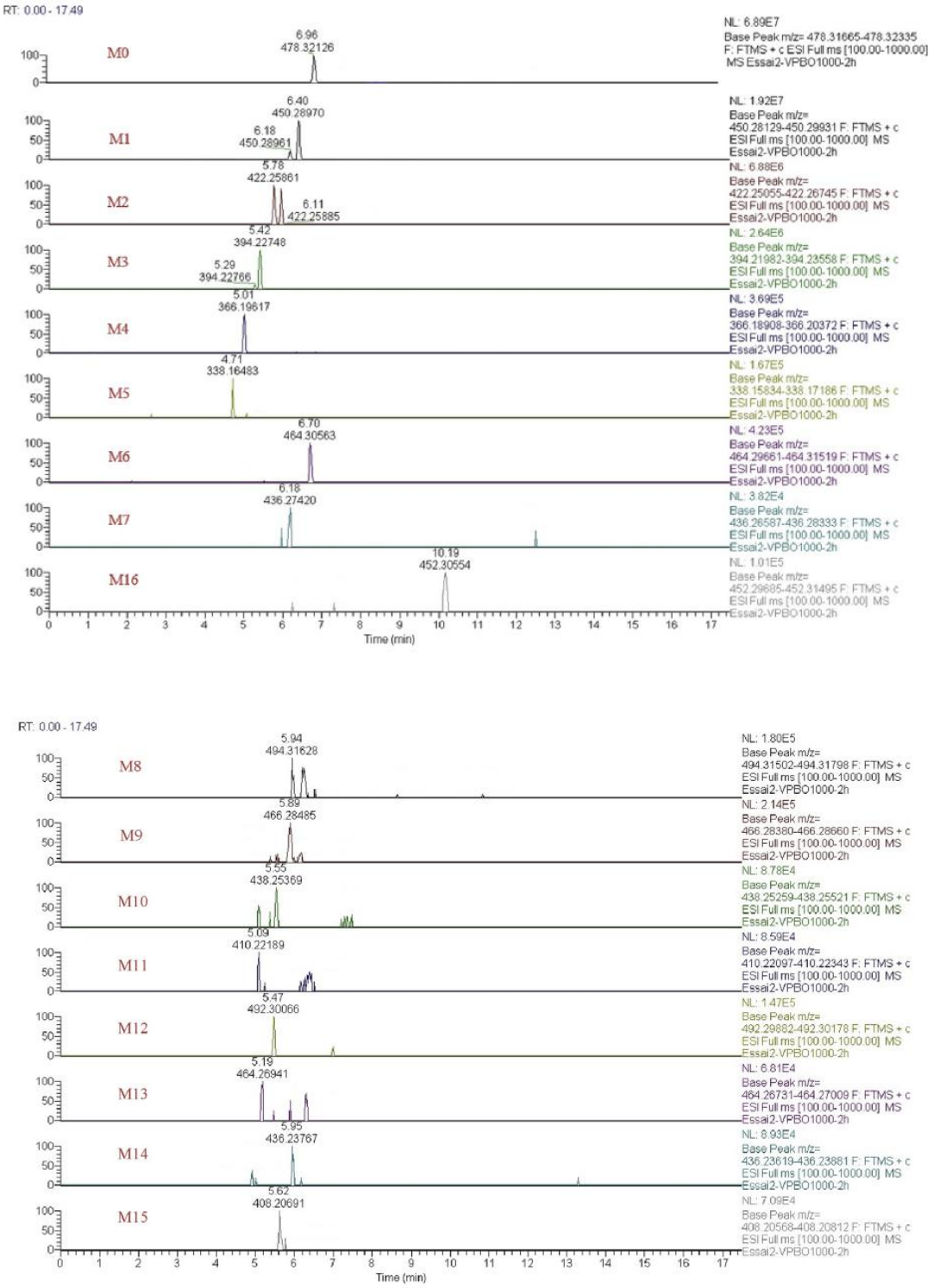

Fig. 2. The extracted ion chromatograms ofVPBO metabolites in trout S9 supernatant after 2 h of incubation.

conversion.

3.3.3. *Phase II metabolism*

In vitro incubation systems with S9 fractions are still used compared with hepatic cell lines to study the reactions of Phase II metabolism in humans (Negreira et al., 2015; Richter et al., 2017); however, these systems are rarely used in fish (Connors et al., 2013). An incubation period of 3 h, based on the methodology of Negreira et al. (2016) was considered sufficient to ensure the formation of conjugated metabolites, in particular when a Phase I reaction must

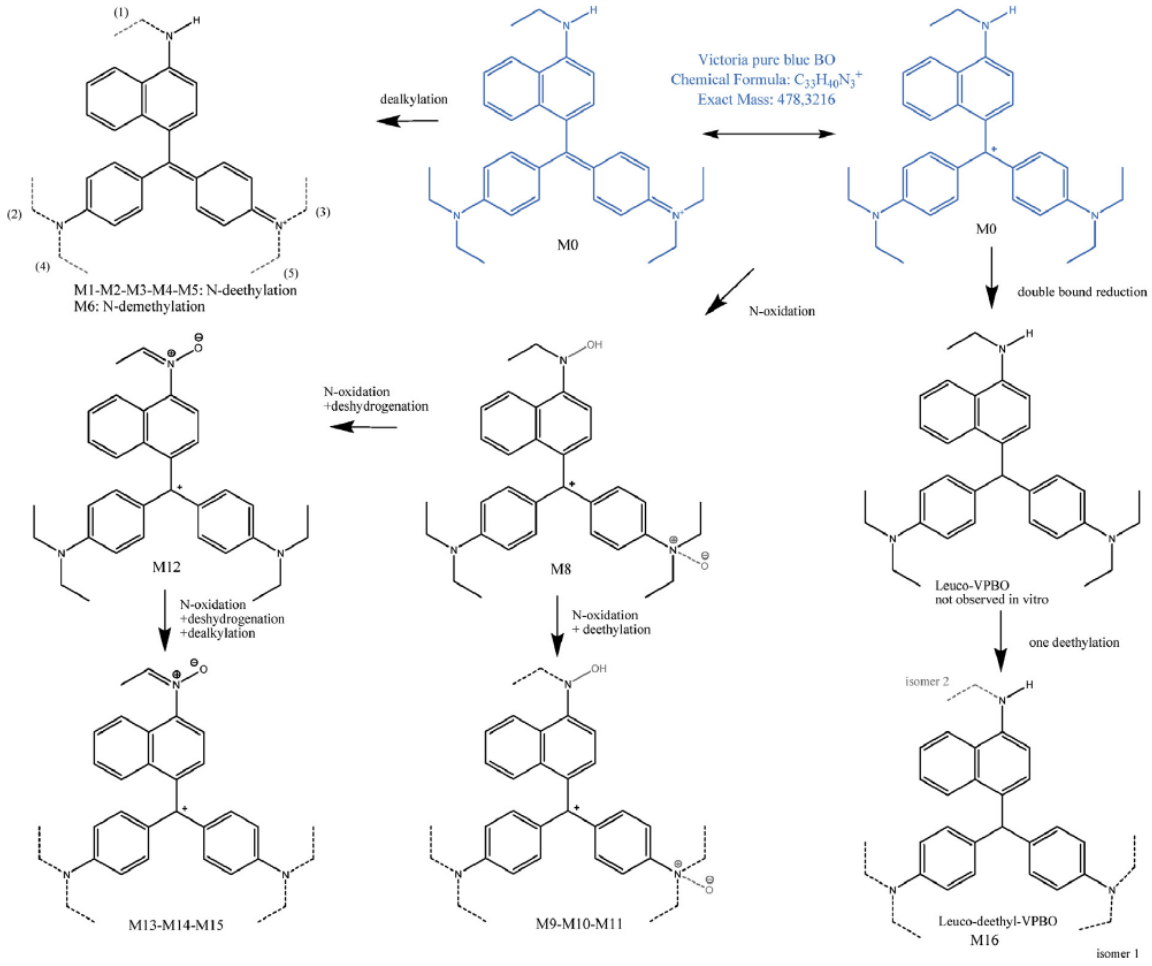

Fig. 3. Putative metabolic pathway of VPBO.

occur just prior to conjugation. Four Phase II activities were tested by incubation with specific substrates: 7-hydroxycoumarine for glucuronidation, apigenine for sulfation, acetaminophen for glutathion conjugation and epinephrine for methylation.

Regarding recoveries, incubation of VPBO or MG substrates with Phase II enzymes separately or simultaneously with Phase I enzymes did not lead to their depletion compared with incubation with only NADPH (see Table 2). Recoveries show that no supplementary depletion of VPBO occurred when adding only one Phase II reaction (recovery of 40% for phase I + glucuronidation, recovery of 59% for phase I + gluthatione conjugation, recovery of 70% for phase I + sulfotransferase conjugation) or simultaneously (recovery of 66%) compared with Phase I reactions only (recovery of 65%). Also, no Phase II conjugates of VPBO or MG were detected in the Phase II experiments. Further, the metabolite of apigenine produced by SULTs (apigenine-7-sulfate), of acetaminophen produced by GSH red (acetaminophen-glutathione) and of 7-hydroxycoumarine produced by UDPGA (7-hydroxycoumarine glucuronide) were detected in the positive control sample, demonstrating good experimental design and suggesting that the three conjugation reactions (sulfation, glutathione, glucuronidation) did not occur for VPBO, unless Phase II metabolites for VPBO cannot be detected by our method or that our method is not sensitive enough. However, the methylation of epinephrine did not lead to the emergence of the o-methylated metabolite metanephrine.

3.4. Confirmation of major metabolite identity

The objective of this in *vitro* study on a triarylmethane derivative was to investigate VPBO metabolism. Incubations with liver microsomal or S9 fractions showed some similarities between the known metabolism of MG and that of VPBO, particularly N-oxidative dealkylation and N-oxidation. The CYP-dependent metabolism, particularly CYP1A, appears to be involved in these reactions as well as in the double bond reduction reaction. Inducing CYP1A with the specific inducer BNF led to a higher production of metabolites (Table 1). On the other hand, the double bond reduction appears to be more difficult to induce *in vitro* for VPBO than for MG.

In this study, a total of 16 VPBO metabolites were detected *in vitro* on trout microsome and S9 fractions. The proposed major metabolic pathway of VPBO is shown in Fig. 3. In regard to our objective of compiling enough metabolism information to propose a potential biomarker for the control of VPBO in farmed fish, we focused on the main metabolite deethyl-VPBO, the one detected with the greatest peak intensity. Our previous metabolomic study including an experiment on trout led to the formation of the deethyl-leuco metabolite after *in vivo* treatment with VPBO, not

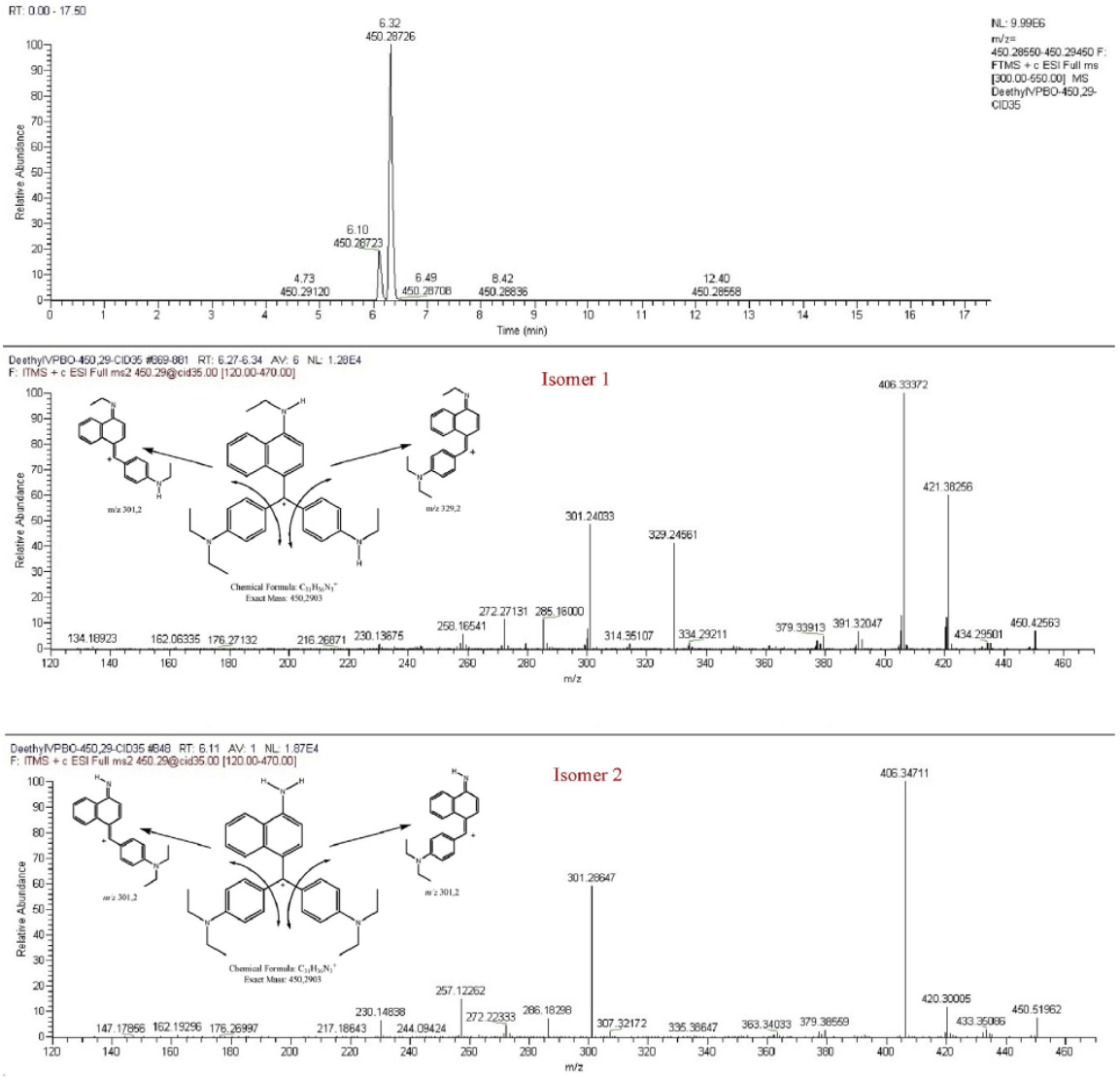

Fig. 4. Proposed structure of deethyl VPBO, XIC and obtained MS/MS CID spectra.

just the deethyl form (Dubreil et al., 2019). This result appears to suggest that deethyl-leuco VPBO is very easily produced in fish, but not in *in vitro* microsomes. In S9 induced fractions, the metabolic deethylation of VPBO led to two positional isomers of similar mass (*m/z* 450.2903) that were further fragmented by CID in the LC-LTQ-Orbitrap-HRMS. Upon deethyl-VPBO fragmentation, isomer 1 produced four fragments (*m/z* 421.3826; 406.3337; 329.2456; 301.2403), whereas isomer 2 produced only two fragments (*m/z* 406.3471; 301.2864). The two fragmentation patterns and proposed structures for deethyl-VPBO isomers are shown in Fig. 4. In addition, a similar CID fragmentation of the parent compound VPBO (data not shown) showed that the most intense isomer (isomer 1, see Fig. 4) of deethyl-VPBO had a similar fragmentation pattern as the ion *m/z* 329.3 from VPBO fragmentation. Given that the fragment ion *m/z* 329.3 is not subject to deethylation, the modification of deethylation for isomer 1 of deethyl-VPBO was carried out on a neutral fragment, i.e. N-deethylaniline. For isomer 2 (see Fig. 4), deethylation occurred on N-ethylnaphtylamine, because fragmentation led to ion *m/z* 301.2 and not ion *m/z* 329.3.

4. Conclusion

Here, we developed an *in vitro* experiment to study the biotransformation of VPBO and MG in fish liver sub-cellular fractions. Our results suggest that the biotransformation of VPBO in fish liver is mediated by CYP enzymes forming both dealkylated metabolites and N-oxidated metabolites as well as a double bond reduction leading to a leuco-form, the deethyl-leuco-VPBO. The single N-deethylation led to a major intense metabolite in this *in vitro* study. In view of these results, the N-deethylated metabolite of VPBO should be a relevant biomarker after a fish treatment bu VPBO and should be included in analytical methods for control of fish foodstuffs. In comparison, the well-known dye of the triarylmethane family, i.e. MG, follows a similar pathway *in vitro* for dealkylation, but not for the N-oxidated metabolites. Furthermore, MG forms several leuco-(dealkylated) metabolites in contrast with VPBO that forms none. The present study demonstrates that CYP1A can be involved in biotransformation of MG and VPBO in fish liver sub-cellular fractions. This study generated the first set of data on

metabolism of a pharmacologically active dye, VPBO, which can be integrated in the chemical residue control for the food safety of aquaculture products in the near future.

Conflicts of interest

Estelle Dubreil and all the authors declare that there is no conflict of interest in regard to their work presented here.

Acknowledgements

This work was financed by the European Union Reference Laboratory for Antibiotic and Dye Residue in Food at the French Agency for Food, Environmental and Occupational Health & Safety (ANSES).

Appendix A. Supplementary data

Supplementary data to this article can be found online at https://doi.org/10.1016/j.chemosphere.2019.124538.

References

Alderman, D.J., 1985. Malachite green: a review. J. Fish Dis. 8, 289–298.
Andersen, W.C., Casey, C.R., Schneider, M.J., Turnipseed, S.B., 2015. Expansion of the scope of AOAC first action method 2012.25 - single-laboratory validation of triphenylmethane dye and leuco metabolite analysis in shrimp, tilapia, catfish, and salmon by LC-MS/MS. J. AOAC Int. 98, 636–648.
Andersen, W.C., Casey, C.R., Nickel, T.J., Young, S.L., Turnipseed, S.B., 2018. Dye residue analysis in raw and processed aquaculture products: matrix extension of AOAC INTERNATIONAL official method 2012.25. J. AOAC Int. 101, 1927–1939.
Anthérieu, S., Chesné, C., Li, R., Camus, S., Lahoz, A., Picazo, L., Turpeinen, M., Tolonen, A., Uusitalo, J., Guguen-Guillouzo, C., Guillouzo, A., 2010. Stable expression, activity, and inducibility of cytochromes P450 in differentiated HepaRG cells. Drug Metab. Dispos. 38, 516–525.
Bumpus, J.A., Brock, B.J., 1988. Biodegradation of crystal violet by the white rot fungus Phanerochaete chrysosporium. Appl. Environ. Microbiol. 54, 1143–1150.
Burka, J.F., Hammell, K.L., Horsberg, T.E., Johnson, G.R., Rainnie, D.J., Speare, D.J., 1997. Drugs in salmonid aquaculture - a review. J. Vet. Pharmacol. Ther. 20, 333–349.
Burkina, V., Zlabek, V., Zamaratskaia, G., 2013. Clotrimazole, but not dexamethasone, is a potent in vitro inhibitor of cytochrome P450 isoforms CYP1A and CYP3A in rainbow trout. Chemosphere 92, 1099–1104.
Burkina, V., Sakalli, S., Pilipenko, N., Zlabek, V., Zamaratskaia, G., 2018. Effect of human pharmaceuticals common to aquatic environments on hepatic CYP1A and CYP3A-like activities in rainbow trout (Oncorhynchus mykiss): an in vitro study. Chemosphere 205, 380–386.
Cha, C.J., Doerge, D.R., Cerniglia, C.E., 2001. Biotransformation of malachite green by the fungus cunninghamella elegans. Appl. Environ. Microbiol. 67, 4358–4360.
EFSA CONTAM Panel, Knutsen, H.K., Alexander, J., Barregård, L., Bignami, M., Brüschweiler, B., Ceccatelli, S., Cottrill, B., Dinovi, M., Edler, L., Grasl-Kraupp, B., Hogstrand, C., Nebbia, C.S., Oswald, I.P., Petersen, A., Rose, M., Roudot, A.-C., Schwerdtle, T., Vollmer, G., Vleminckx, C., Wallace, H., Filipič, M., Fürst, P., O'Keeffe, M., Penninks, A., Van Leeuwen, R., Baert, K., Hoogenboom, L., 2018. Update: methodological principles and scientific methods to be taken into account when establishing Reference Points for Action (RPAs) for non-allowed pharmacologically active substances present in food of animal origin. EFSA J. 16, e05332.
Connors, K.A., Du, B., Fitzsimmons, P.N., Hoffman, A.D., Chambliss, C.K., Nichols, J.W., Brooks, B.W., 2013. Comparative pharmaceutical metabolism by rainbow trout (Oncorhynchus mykiss) liver S9 fractions. Environ. Toxicol. Chem. 32, 1810–1818.
Culp, S.J., Blankenship, L.R., Kusewitt, D.F., Doerge, D.R., Mulligan, L.T., Beland, F.A., 1999a. Toxicity and metabolism of malachite green and leucomalachite green during short-term feeding to Fischer 344 rats and B6C3F1 mice. Chem. Biol. Interact. 122, 153–170.
Culp, S.J., Blankenship, L.R., Kusewitt, D.F., Doerge, D.R., Mulligan, L.T., Beland, F.A., 1999b. Toxicity and metabolism of malachite green and leucomalachite green during short-term feeding to Fischer 344 rats and B6C3F$_1$mice. Chem. Biol. Interact. 122, 153–170.
Doerge, D.R., Churchwell, M.I., Gehring, T.A., Pu, Y.M., Plakas, S.M., 1998. Analysis of malachite green and metabolites in fish using liquid chromatography atmospheric pressure chemical ionization mass spectrometry. Rapid Commun. Mass Spectrom. 12, 1625–1634.
Dubreil, E., Mompelat, S., Kromer, V., Guitton, Y., Danion, M., Morin, T., Hurtaud-Pessel, D., Verdon, E., 2019. Dye residues in aquaculture products: targeted and metabolomics mass spectrometric approaches to track their abuse. Food Chem. 294, 355–367.
Fallah, A.A., Barani, A., 2014. Determination of malachite green residues in farmed rainbow trout in Iran. Food Control 40, 100–105.
Ferron, P.J., Hogeveen, K., De Sousa, G., Rahmani, R., Dubreil, E., Fessard, V., Le Hegarat, L., 2016. Modulation of CYP3A4 activity alters the cytotoxicity of lipophilic phycotoxins in human hepatic HepaRG cells. Toxicol. In Vitro 33, 136–146.
Foster, F.J., Woodbury, L., 1936. The use of malachite green as a fish fungicide and antiseptic. Progressive Fish-Culturist 3, 7–9.
Gräslund, S., Bengtsson, B.E., 2001. Chemicals and biological products used in south-east Asian shrimp farming, and their potential impact on the environment - a review. Sci. Total Environ. 280, 93–131.
Guengerich, F.P., 1992. Cytochrome P450: advances and prospects. FASEB (Fed. Am. Soc. Exp. Biol.) J. 6, 667–668.
Hashimoto, J.C., Paschoal, J.A.R., De Queiroz, J.F., Reyes, F.G.R., 2011. Considerations on the use of malachite green in aquaculture and analytical aspects of determining the residues in fish: a review. J. Aquat. Food Prod. Technol. 20, 273–294.
Holčapek, M., Kolářová, L., Nobilis, M., 2008. High-performance liquid chromatography-tandem mass spectrometry in the identification and determination of phase i and phase II drug metabolites. Anal. Bioanal. Chem. 391, 59–78.
Ikenaka, Y., Oguri, M., Saengtienchai, A., Nakayama, S.M.M., Ijiri, S., Ishizuka, M., 2013. Characterization of phase-II conjugation reaction of polycyclic aromatic hydrocarbons in fish species: unique pyrene metabolism and species specificity observed in fish species. Environ. Toxicol. Pharmacol. 36, 567–578.
James, M.O., Stuchal, L.D., Nyagode, B.A., 2008. Glucuronidation and sulfonation, in vitro, of the major endocrine-active metabolites of methoxychlor in the channel catfish, Ictalurus punctatus, and induction following treatment with 3-methylcholanthrene. Aquat. Toxicol. 86, 227–238.
Jönsson, M.E., Gao, K., Olsson, J.A., Goldstone, J.V., Brandt, I., 2010. Induction patterns of new CYP1 genes in environmentally exposed rainbow trout. Aquat. Toxicol. 98, 311–321.
Lewis, D.F.V., 2004. 57 varieties: the human cytochromes P450. Pharmacogenomics 5, 305–318.
Lněničková, K., Skálová, L., Stuchlíková, L., Szotáková, B., Matoušková, P., 2018. Induction of xenobiotic-metabolizing enzymes in hepatocytes by beta-naphthoflavone: time-dependent changes in activities, protein and mRNA levels. Acta Pharm. 68, 75–85.
Nabb, D.L., Mingoia, R.T., Yang, C.H., Han, X., 2006. Comparison of basal level metabolic enzyme activities of freshly isolated hepatocytes from rainbow trout (Oncorhynchus mykiss) and rat. Aquat. Toxicol. 80, 52–59.
Negreira, N., Erratico, C., Kosjek, T., van Nuijs, A.L., Heath, E., Neels, H., Covaci, A., 2015. In vitro Phase I and Phase II metabolism of α-pyrrolidinovalerophenone (α-PVP), methylenedioxypyrovalerone (MDPV) and methedrone by human liver microsomes and human liver cytosol. Anal. Bioanal. Chem. 407, 5803–5816.
Negreira, N., Erratico, C., van Nuijs, A.L.N., Covaci, A., 2016. Identification of in vitro metabolites of ethylphenidate by liquid chromatography coupled to quadrupole time-of-flight mass spectrometry. J. Pharm. Biomed. Anal. 117, 474–484.
Penninks, A., Baert, K., Levorato, S., Binaglia, M., 2017. Dyes in aquaculture and reference points for action. EFSA J. 15, e04920.
Plakas, S.M., El Said, K.R., Stehly, G.R., Gingerich, W.H., Allen, J.L., 1996. Uptake, tissue distribution, and metabolism of malachite green in the channel catfish [Ictalurus punctatus]. Can. J. Fish. Aquat. Sci. 53, 1427–1433.
RASFF-portal. European commission. https://webgate.ec.europa.eu/rasff-window/portal/.
Ren, W., Li, Y., Zuo, R., Wang, H.J., Si, N., Zhao, H.Y., Han, L.Y., Yang, J., Bian, B.L., 2014. Species-related difference between limonin and obacunone among five liver microsomes and zebrafish using ultra-high-performance liquid chromatography coupled with a LTQ-Orbitrap mass spectrometer. Rapid Commun. Mass Spectrom. 28, 2292–2300.
Reyns, T., Belpaire, C., Geeraerts, C., Van Loco, J., 2014. Multi-dye residue analysis of triarylmethane, xanthene, phenothiazine and phenoxazine dyes in fish tissues by ultra-performance liquid chromatography-tandem mass spectrometry. J. Chromatogr. B Analyt. Technol. Biomed. Life Sci. 953–954, 92–101.
Richter, L.H.J., Flockerzi, V., Maurer, H.H., Meyer, M.R., 2017. Pooled human liver preparations, HepaRG, or HepG2 cell lines for metabolism studies of new psychoactive substances? A study using MDMA, MDBD, butylone, MDPPP, MDPV, MDPB, 5-MAPB, and 5-API as examples. J. Pharm. Biomed. Anal. 143, 32–42.
Sakalli, S., Burkina, V., Pilipenko, N., Zlabek, V., Zamaratskaia, G., 2018. In vitro effects of diosmin, naringenin, quercetin and indole-3-carbinol on fish hepatic CYP1A1 in the presence of clotrimazole and dexamethasone. Chemosphere 192, 105–112.
Schneider, K., Hafner, C., Jäger, I., 2004. Mutagenicity of textile dye products. J. Appl. Toxicol. 24, 83–91.
Schneider, M.J., Andersen, W.C., 2015. Determination of triphenylmethane dyes and their metabolites in salmon, catfish, and shrimp by LC-MS/MS using AOAC first action method 2012.25: collaborative study. J. AOAC Int. 98, 658–670.
Shen, M., Cheng, J., Wu, R., Zhang, S., Mao, L., Gao, S., 2012. Metabolism of polybrominated diphenyl ethers and tetrabromobisphenol A by fish liver subcellular fractions in vitro. Aquat. Toxicol. 114–115, 73–79.
Singh, S., Das, M., Khanna, S.K., 1994. Biodegradation of malachite green and rhodamine B by cecal microflora of rats. Biochem. Biophys. Res. Commun. 200, 1544–1550.
Smith, P.K., Krohn, R.I., Hermanson, G.T., Mallia, A.K., Gartner, F.H., Provenzano, M.D., Fujimoto, E.K., Goeke, N.M., Olson, B.J., Klenk, D.C., 1985. Measurement of protein using bicinchoninic acid. Anal. Biochem. 150, 76–85.

Smith, E.M., Iftikar, F.I., Higgins, S., Irshad, A., Jandoc, R., Lee, M., Wilson, J.Y., 2012. In vitro inhibition of cytochrome P450-mediated reactions by gemfibrozil, erythromycin, ciprofloxacin and fluoxetine in fish liver microsomes. Aquat. Toxicol. 109, 259–266.

Srivastava, S., Sinha, R., Roy, D., 2004. Toxicological effects of malachite green. Aquat. Toxicol. 66, 319–329.

Tao, Y., Chen, D., Chao, X., Yu, H., Yuanhu, P., Liu, Z., Huang, L., Wang, Y., Yuan, Z., 2011. Simultaneous determination of malachite green, gentian violet and their leuco-metabolites in shrimp and salmon by liquid chromatography-tandem mass spectrometry with accelerated solvent extraction and auto solid-phase clean-up. Food Control 22, 1246–1252.

Tarbin, J.A., Chan, D., Stubbings, G., Sharman, M., 2008. Multiresidue determination of triarylmethane and phenothiazine dyes in fish tissues by LC-MS/MS. Anal. Chim. Acta 625, 188–194.

Thompson Jr., H.C., Rushing, L.G., Gehring, T., Lochmann, R., 1999. Persistence of gentian violet and leucogentian violet in channel catfish (ictalurus punctatus) muscle after water-borne exposure. J. Chromatogr. B Biomed. Sci. Appl. 723, 287–291.

Turnipseed, S.B., Andersen, W.C., Roybal, J.E., 2005. Determination and confirmation of malachite green and leucomalachite green residues in salmon using liquid chromatography/mass spectrometry with no-discharge atmospheric pressure chemical ionization. J. AOAC Int. 88, 1312–1317.

Vestergren, A.S., Zlabek, V., Pickova, J., Zamaratskaia, G., 2012. Tolbutamide hydroxylation by hepatic microsomes from Atlantic salmon (Salmo salar L.). Mol. Biol. Rep. 39, 6867–6873.

Villar-Pulido, M., Gilbert-Lopez, B., Garcia-Reyes, J.F., Martos, N.R., Molina-Diaz, A., 2011. Multiclass detection and quantitation of antibiotics and veterinary drugs in shrimps by fast liquid chromatography time-of-flight mass spectrometry. Talanta 85, 1419–1427.

WHO/FAO, 2015. Maximum Residue Limits (MRLs) and Risk Management Recommendations (RMRs) for Residues of Veterinary Drugs in Foods. CAC/MRL 2-2015-Updated as at the 38th Session of the Codex Alimentarius Commission (July 2015).

Zhang, Y., Sun, Y., Mu, X., Yuan, L., Wang, Q., Zhang, L., 2017. Identification of metabolites of vindoline in rats using ultra-high performance liquid chromatography/quadrupole time-of-flight mass spectrometry. J. Chromatogr. B: Anal. Technol. Biomed. Life Sci. 1060, 126–137.

Zlabek, V., Burkina, V., Borrisser-Pairó, F., Sakalli, S., Zamaratskaia, G., 2016. Phase I metabolism of 3-methylindole, an environmental pollutant, by hepatic microsomes from carp (Cyprinus carpio) and rainbow trout (Oncorhynchus mykiss). Chemosphere 150, 304–310.

Article 3 : Tissue distribution, metabolism, and elimination of the dye Victoria pure blue lead to an appropriate biomarker in trout

1.1 Contexte

Une précédente étude de métabolomique *in vivo* chez la truite arc-en-ciel traitée (article 1) a conduit à la découverte de certains marqueurs d'acide biliaire endogènes ainsi que de deux métabolites du VPBO, le DLVPBO et le tri-dééthyl-VPBO (Dubreil et al., 2019b, 2020a). L'étude *in vitro*, quant-à-elle, a mis en évidence l'apparition de nombreux métabolites, dont un majeur, le dééthyl-VPBO (article 2). Nous avons mis en place une étude de pharmacocinétique avec une déplétion sur deux mois chez la truite arc-en-ciel (*Oncorhinchus mykiss*), afin de définir plus précisément un résidu marqueur. L'expérimentation a été conduite à l'Anses de Plouzané dans l'Unité Pathologies Virales des Poissons, comme pour l'étude de métabolomique.

Les objectifs étaient (1) d'identifier le principal métabolite du VPBO dans la truite arc-en-ciel traitée; (2) de caractériser la distribution tissulaire de VPBO et de son principal métabolite trouvé dans la truite arc-en-ciel traitée pendant les périodes d'absorption et de dépuration; (3) d'estimer et de comparer les temps de demi-vie du VPBO et de son principal métabolite dans les muscles et la peau; et (4) de suggérer un résidu marqueur dans les tissus comestibles (muscle + peau) pour des évaluations appropriées en sécurité sanitaire des aliments.

1.2 Méthodologie et principaux résultats

Méthodologie de la phase animale :

Traitement et dépuration : Le colorant a été administré à la truite arc-en-ciel pendant une journée au bain-marie en circuit fermé à une dose de 0,1 mg.L^{-1}. Le système a été ensuite positionné en circuit ouvert pendant environ deux mois pour l'étude de la dépuration du VPBO.

Pendant ces périodes, 6 poissons étaient prélevés:

- Durant le traitement à: 0.083, 0.25, 0.417 et 1 jour.

- Durant la dépuration à: 2, 3, 5, 9, 17, 34, 49 et 65 jours.

Méthodologie de recherche d'un résidu marqueur :

Le principe de cette approche était d'analyser les signaux obtenus après extraction des tissus de poisson et analyse LC-HRMS, afin de les exploiter par des modèles de pharmacocinétique pour le VPBO et un métabolite majeur identifié. Le VPBO a été dosé par une méthode validée puis la concentration du métabolite majeur identifié, le DLVPBO, a été estimée en considérant une équivalence de signal avec le parent. L'exploitation pharmacocinétique a été réalisée pour les tissus cibles de muscle et de peau. Un modèle non-compartimental a été appliqué pour déterminer les paramètres de pharmacocinétique.

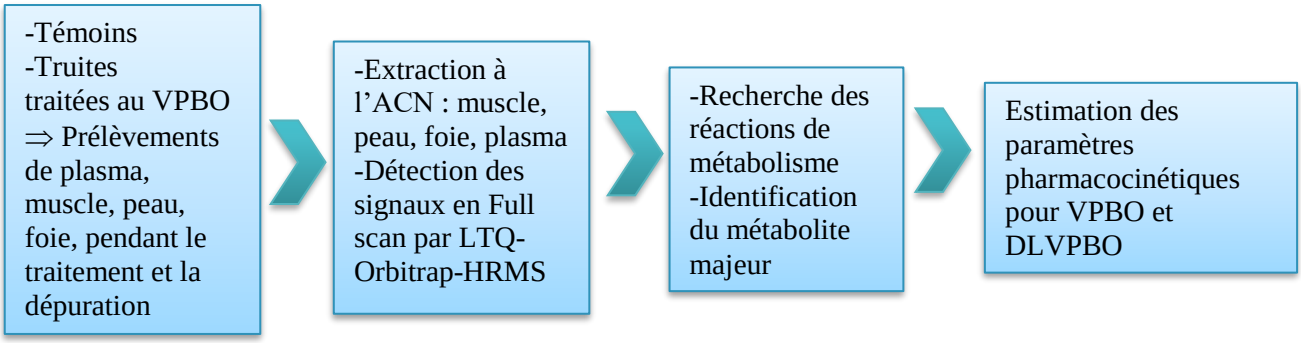

Principaux résultats :

Objectifs : identifier le métabolite majeur, appréhender la pharmacocinétique du VPBO chez la truite arc-en-ciel. Proposer un résidu marqueur de traitement.

Phase animale, prélèvements et extraction des tissus

Recherche des métabolites formés

-Méthode validée pour le dosage du VPBO dans le muscle, la peau, le foie, le plasma.
-Détection de 15 métabolites, dont 14 métabolites de phase I proposés et 1 de phase II
-Le DLVPBO identifié comme métabolite majeur dans le muscle et la peau de truite.

Dosage du VPBO dans les tissus
Pharmacocinétique du VPBO et DLVPBO

-VPBO :
Traitement :
Foie>peau>muscle>plasma
Dépuration :
Conc. VPBO > LOQ dans muscle et peau
Demi-vie élimination= 17.1 jours muscle
Temps de résidence moyen : 12.7 jours peau et 20.7 jours muscle

-DLVPBO :
Dépuration :
Cmax DLVPBO < Cmax VPBO muscle et peau
Demi-vie élimination= 22.5 jours muscle
Temps de résidence moyen : 29.9 jours peau et 43.1 jours muscle

1.3 Conclusion

A notre connaissance, aucune étude pharmacocinétique n'a jamais été réalisée sur le composé VPBO chez les poissons. Nous avons pu montrer que le VPBO est rapidement absorbé et distribué dans le muscle, la peau, et le foie après une administration dans l'eau du bassin pendant un jour. Nous avons identifié l'apparition de 15 métabolites, dont 14 de phase I et un de phase II proposé. Ces métabolites, excepté celui de phase II, sont similaires à ceux détectés *in vitro*. Le dééthyl-leuco-VPBO, identifié auparavant pendant l'étude de métabolomique, a été déterminé comme le plus intense et le plus persistant sur la période de dépuration de 2 mois dans les tissus. Bien que les concentrations du VPBO soient supérieures à celles du DLVPBO au début du traitement, elles tombent en-dessous celle du DLVPBO au bout de 17 jours de dépuration dans le muscle et la peau. Nous avons pu démontré qu'au bout de 60 jours de traitement, les concentrations de VPBO et son métabolite majeur, le DLVPBO, sont encore détectables dans le muscle et la peau. Le DLVPBO semble légèrement (environ 3 fois) plus intense que son parent à la fin de cette période. Ces résultats démontrent que le VPBO et son métabolite majeur, le DLVPBO, devraient être suivis dans les tissus comestibles de poisson. Le DLVPBO est un résidu marqueur approprié car il est plus persistant, et le VPBO est plus intense dans la première partie du traitement. C'est pourquoi la surveillance de ces deux résidus ne doit pas être dissociée pour un contrôle efficace des résidus.

Chemosphere 262 (2021) 127636

Contents lists available at ScienceDirect

Chemosphere

journal homepage: www.elsevier.com/locate/chemosphere

Tissue distribution, metabolism, and elimination of Victoria Pure Blue BO in rainbow trout: Main metabolite as an appropriate residue marker

Estelle Dubreil [a, *], Michel Laurentie [a], Jean-Michel Delmas [a], Morgane Danion [b], Thierry Morin [b], Dominique Hurtaud-Pessel [a], Alexis Viel [a], Pascal Sanders [a], Eric Verdon [a]

[a] Laboratory of Fougères, French Agency for Food, Environmental and Occupational Health & Safety, ANSES, Fougères, France
[b] Laboratory of Ploufragan-Plouzané-Niort, French Agency for Food, Environmental and Occupational Health & Safety, ANSES, Ploufragan-Plouzané-Niort, France

HIGHLIGHTS

- The metabolism of Victoria Pure Blue BO (VPBO) was investigated in rainbow trout.
- Residues were detected by LC-HRMS in muscle, plasma, skin, and liver.
- The half-lives of VPBO and the main metabolite were assessed.
- Deethyl-leuco-VPBO is proposed as a marker of exposure to VPBO in rainbow trout.

GRAPHICAL ABSTRACT

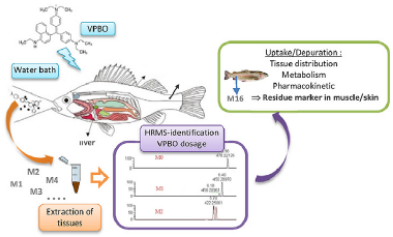

ARTICLE INFO

Article history:
Received 29 April 2020
Received in revised form
3 July 2020
Accepted 5 July 2020
Available online 17 July 2020

Handling Editor: David Volz

Keywords:
Mass spectrometry
Fish metabolism
Dyes
Treatment
Depuration
Kinetics

ABSTRACT

Victoria Pure Blue BO is a dye that bears some therapeutic activity and that can be retrieved in effluent or may be used in aquaculture as a prohibited drug. In this study, the metabolism and tissue distribution during uptake and depuration of VPBO were investigated in order to propose a residue marker of illegal treatment in fish. The dye was administered to rainbow trout (*oncorhynchus mykiss*) for one day by water bath at a dose of 0.1 mg.L^{-1}. The concentrations of VPBO in all tissues increased rapidly during the treatment period, reaching a C_{max} of 567 ± 301 µg.L^{-1} in plasma and 1846 µg kg^{-1} ±517 for liver after 2 h. After placing the rainbow trout in a clean water bath for a 64 day-period of depuration, the concentrations in the tissues and plasma decreased to reach comparable levels for muscle and for skin after 33 days. The concentrations measured were still above the LOQ at 2.26 ± 0.48 µg kg^{-1} for muscle and 2.85 ± 1.99 µg kg^{-1} for skin at the end of the depuration period. The results indicated the existence of 14 phase I metabolites and one glucuronide conjugated metabolite. Non-compartmental analysis was applied to assess the pharmacokinetic parameters. The half-life in edible muscle of the main metabolite detected, deethyl-leuco-VPBO, was found to be 22.5 days compared to a half-life of 19.7 days for the parent VPBO. This study provides new information to predict a VPBO drug treatment of aquacultured species via a proposed new residue marker.

* Corresponding author.
E-mail address: estelle.dubreil@anses.fr (E. Dubreil).

https://doi.org/10.1016/j.chemosphere.2020.127636
0045-6535/

1. Introduction

Victoria Pure Blue BO (VPBO), also known as Basic blue 7, is a dye that was found in contaminated panga fish (*pangasius bocourti*) imported from Vietnam in 2010. The contamination was reported in Europe via the Rapid Alert System for Food and Feed (RASFF) managed by the European Union (notification 2010.1372) (RASFF-portal, European Commission). The contamination could have originated from environmental effluent waste because Basic blue 7 is commonly used in the industry to dye certain textiles (Gessner and Mayer, 2000). Alternatively, it could have come from intentional and illegal treatment in aquaculture. The efficacy of the substance has not been proven in aquaculture, but it has been demonstrated in the past that it could bear some therapeutic activity. A research team (Alderman, 1982) developed *in vitro* tests to determine the efficacy of 11 therapeutic triarylmethane dyes, including VPBO, against the parasitic fungi *Saprolegnia parasitica* in fish. In a recent report issued by the European Food Safety Authority (EFSA), VPBO was classified as potentially genotoxic, along with 19 other dyes, due to a lack of knowledge regarding its genotoxicity (ECHA; EFSA et al., 2017). VPBO has been found to efficiently bind to DNA and to mediate its photochemical destruction in tumor cells (Lewis and Indig, 2001, 2002). Based on this isolated information and modeling using a quantitative structure-activity relationship (QSAR) approach, EFSA concluded that VPBO should be considered genotoxic (EFSA et al., 2017). The dye was assigned to group I on the basis of a decision tree applying a toxicological screening value (TSV) of 0.0025 μg kg $^{-1}$ body weight per day (EFSA et al., 2017). This TSV could serve as a basis in the near future if EFSA sets a Reference Point for Action (RPA), an action limit related to illegal veterinary drugs found in animal food products. The suspicion of toxicity was recently underpinned by a study within the framework of the Tox21 national program in the United States. The toxicity of 10,000 chemicals has been studied in 70 different cell tests covering more than 200 cells signaling pathways. While MG is ranked among the 30 most active drugs, VPBO (basic blue 7) is the most active compound among environmental contaminants (Ngan et al., 2019). In addition, the structure of VPBO, a cationic dye derived from the family of triarylmethanes by the replacement of an aryl group and methyl groups by a naphthyl group and ethyl groups, respectively, may result in certain physicochemical properties associated to the well-known compounds Malachite Green (MG) and Crystal Violet (CV). Probably the most widely used of these chemicals is MG, which is the most popular fungicide in farmed and pet fish and is also effective against ectoparasites in certain protozoan parasite conditions (Alderman, 1985; Srivastava et al., 2004). Since MG and its major metabolite Leuco-Malachite Green (LMG) have several toxic effects in mammalian cells, MG has never been registered as a veterinary medicinal product in the European Union; this is also the case for Crystal Violet. The United States Food and Drug Administration has also not approved any use of these dyes (Culp et al., 1999; Srivastava et al., 2004; Verdon et al., 2015). Despite their toxicity in humans and fish, MG and CV are still used worldwide, probably because no other pharmaceutical drugs have proven to be as effective, and too few therapeutic treatments are currently approved in fish farming (Schnick, 1988; Sudova et al., 2007; Okocha et al., 2018). It has been found that illegal drugs are sometimes replaced by similar illegal drugs or cocktails of these substances (Dervilly-Pinel et al., 2015; Gallart-Ayala et al., 2015).

Although LMG is the main residue marker of MG illegal treatment in aquaculture practices, no residue marker has ever been defined for the Victoria dye family and in particular, for VPBO. A previous *in vitro* study in rainbow trout involving incubation of subcellular fractions with dyes suggested that the main metabolite would be deethyl-VPBO (Dubreil et al., 2020b). A previous *in vivo* metabolomics study in treated rainbow trout led to the discovery of certain endogenous bile acid markers and also two VPBO metabolites (Dubreil et al., 2019b, 2020a). To the best of our knowledge, no pharmacokinetic study has ever been carried out on the VPBO compound in fish. However, a few studies described the pharmacokinetics of MG and LMG. MG is rapidly absorbed in different fish species, partly depending on the pH and water temperature in ponds, and it is reduced to its leucoform (LMG) that remains in tissues for long periods (Alderman and Clifton-Hadley, 1993; Máchová et al., 1996; Plakas et al., 1996; Bergwerff et al., 2004; Jiang et al., 2009; Bajc et al., 2011; Kwan et al., 2020).

In order to provide information for food control, the present study was performed in rainbow trout to determine the appropriate residue marker after waterborne exposure to VPBO. The objectives were (1) to identify the main metabolite of VPBO in treated rainbow trout; (2) to characterize the tissue distribution of VPBO and its main metabolite found in treated rainbow trout during the uptake and depuration periods; (3) to estimate and compare the half-lives of VPBO and its major metabolite in muscle and skin; and (4) to suggest a residue marker in edible tissue (muscle + skin) for appropriate food safety assessments.

2. Materials and methods

2.1. Reagents and analytical standards

The standard substances Victoria Pure Blue BO (VPBO), and internal standard (IS) Malachite Green-d_5 (MG-d_5), were purchased from Sigma-Aldrich (Europe). The IS Crystal Violet-d_6 (CV-d_6) was obtained from WITEGA (Berlin, Germany). MG-d_5 was used to correct the peak area of MG and CV-d_6 for VPBO. For the analytical assay, a stock solution of VPBO was prepared at 100 μg mL $^{-1}$ in methanol (not dedicated to the animal study). Stock solutions were further diluted to obtain several concentrations ranging from 0.01 μg mL $^{-1}$ to 1 μg mL $^{-1}$. The internal standards were prepared at 0.1 mg mL $^{-1}$ in acetonitrile. For the rainbow trout experiment, a stock solution of VPBO was prepared at 1000 μg mL $^{-1}$ in water.

Acetonitrile, methanol, ammonium acetate, and formic acid were of the appropriate analytical grade (HPLC grade). Water was purified using a Milli-Q system (Millipore, Taunton, MA, USA).

2.2. Experimental study design

This study was conducted in order to evaluate the uptake and depuration kinetics of the parent compound and its major metabolites.

A total of 100 specific pathogen-free rainbow trout including a mixture of males and females from the same genetic group were used in this experiment. They were handled at the protected and monitoring facilities of the ANSES Plouzané laboratory site (France). The fishes in the study batch were one year old, with a weight of 105 ± 25 g and length of 15 ± 2 cm. They were fed with commercial dry pellets at 1.5% body weight (Neo Prima 4, Le Gouessant Aquaculture, France) once a day.

The experimental tank of 400 L was maintained in an open circuit with purified fresh river water at a flow rate of 0.3 m^3 h^{-1} (temperature 13 ± 1 °C, dissolved oxygen < 90%, pH close to 8, and free of nitrates and nitrites) throughout the experiment. The tank was maintained in a natural light/dark cycle (14 h/10 h in spring, approximately) in a room with an air volume change every hour.

After one week in acclimation, 20 control fishes free of exposure were collected and euthanized to obtain blank matrices. The system was then positioned in a closed-circuit configuration where the tank was exposed to 0.1 mg.L $^{-1}$ of VPBO by adding 40 mL of a standard solution dissolved in water at 1 g.L $^{-1}$ into the tank (dose of

40 mg.kg ^{1} b. w. Of VPBO). After a 24-h accumulation period, the fishes were transferred to a new tank, for a 64-day depuration period in a purified fresh river water open circuit.

Six fishes were randomly sampled at several sampling dates:

- during the 24-h exposure period at: 0.083, 0.25, 0.417 and 1 day.
- post treatment during the depuration period at 2, 3, 5, 9, 17, 34, 49 and 65 days.

For each fish, 1 mL of blood was withdrawn from the caudal vein by means of a lithium heparinized vacutainer (BD Vacutainer LH 85 IU). Whole blood samples were centrifuged (1200×g, 10 min, 4 °C) and plasma was stored at −80 °C. Fishes were euthanized after collecting blood by percussive stunning with a head blow, and were then measured and weighed. Liver and muscles with skin were removed and stored at −80 °C for future analysis. Skin was separated from muscle before freezing. The European Medicines Agency (EMA) has indicated that the target tissue considered appropriate for Salmonidae is muscle including the skin, in natural proportions, as the edible tissue in fish. However, for the purposes of food safety assessments for prohibited drugs, it was decided to separate muscle and skin to have a clear picture of contamination in individual tissues (CVMP, 1998).

This study was approved by the French Ethics Committee No.16, reference number 12222−201,711,161,618,463.

2.3. Sample preparation for the study of VPBO in muscle, plasma, skin, and liver

Samples were weighed (2 g of mixed muscle, 200 µL of plasma, 200 mg of mixed skin, 200 mg of mixed liver) and transferred to a centrifuge tube. Then 100 µL for muscle or 10 µL for plasma, skin, and liver of the internal standard solutions (MG-d_5 and CV-d_6 at 50 µg.L ^{1} in acetonitrile) were added. The sample was vortex-mixed and left to stand for 10 min in the dark. Then, acetonitrile was added: 8 mL for muscle, 1 mL for plasma, skin, and liver). The sample was vortex-mixed to homogenize the material with the solvent. The sample was further placed on a mechanical rotary shaker for 15 min at 100 rpm, and then placed in an ultrasound bath for 5 min at 20 °C ± 2 °C. Samples were centrifuged for 10 min at 20,000×g refrigerated at 4 °C. The supernatant was transferred to a polypropylene tube and evaporated to dryness under gentle nitrogen flow at 50 °C. The dry extracts was dissolved by ultrasound in acetonitrile/water for reconstitution (80/20, v/v) (500 µL for muscle, 200 µL for plasma, skin, and liver), and vortex-mixed. The residue for muscle was extracted through a 0.45 µm syringe PVDF filter, and the residues for the other matrices were extracted by centrifugation for 5 min at 20,000×g refrigerated at +4 °C. The samples were transferred to LC vials.

2.4. Liquid chromatography-high resolution mass spectrometry analysis

The investigation of metabolism was conducted in two steps: first the concentration of the parent compound was measured via a quantitative LC-HRMS method, and then the formation of metabolites was studied via the metabolite research software MetWorks®. Chromatography was performed on a Thermofisher U-HPLC Accela system (Bremen, Germany), fitted with a Phenomenex Luna C18 (2) column (Phenomenex, Torrance, CA, USA) (150 × 2.0 mm, 3 µm). The final reconstitution solution for samples after extraction was prepared by mixing 80% acetonitrile with 20% water. Chromatographic separation was carried out using two mobile phase preparations, consisting of mobile phase (A), a mixture of ammonium acetate 10 mM.L ^{1} and 0.1% formic acid, and mobile phase (B), 100% acetonitrile. The gradient conditions were as follows: from 0 to 4 min, ramp up linearly from 98 to 2% of mobile phase A and hold for 4 min, then ramp back over 0.1 min to initial conditions and hold for 4 min to re-equilibrate the system. The flow rate was set at 0.2 mL min ^{1}, the injection volume was 10 µL, and the column oven was maintained at 25 °C. The LTQ Orbitrap XL mass spectrometer (Thermofisher, Bremen, Germany) was operated with an electrospray ionization probe in positive mode, using the following source parameters: sheath gas flow rate: 30 arb; auxiliary gas flow rate: 10 arb; sweep gas flow rate: 2 arb; ion spray voltage: 5 kV; capillary temperature: 275 °C; capillary voltage: 35 V; and tube lens: 90 V. The instrument was calibrated using the manufacturer's calibration solution, to reach mass accuracies in the 1−3 ppm range. The instrument was operated in full-scan mode from m/z 100−1,000, at a resolving power of 60,000 (full width at half maximum), allowing VPBO detection as $VPBO^{+}$ ions, as well as metabolite formation investigations using the metabolism software MetWorks 1.3.0. SP1 (Thermo Fisher Scientific, Waltham, MA, USA). Exact masses of the peaks detected by this software were extracted with a mass window of 5 ppm around the ionized precursor ion, to confirm or discard their identity. For confirmation of the identity of the major metabolite (deethyl-leuco-VPBO), MS^2 mass fragmentation of the compound was performed in the LTQ-Orbitrap mass analyser. The energy for collision-induced dissociation (CID) were set at 35 eV and 70 eV, with an isolation width of m/z 1.

2.5. Validation of the analytical method for VPBO

Calibration curves were prepared by spiking muscle, plasma, skin, and liver prior extraction with VPBO, with the following concentrations: 0.5, 1, 5, 10, and 50 µg kg ^{1}. These calibration samples were prepared and analyzed in duplicate on three different days for muscle, and 1 day each for plasma, skin, and liver to combine the three series. This protocol was chosen in order to select the most appropriate response function. The validation standards were reconstituted samples with matrix containing known concentrations of the analyte of interest. These were prepared at three levels of concentration corresponding to low (estimated limit of quantification), intermediate, and high concentrations levels: 0.5, 5 and 50 µg kg ^{1} of VPBO. These validation samples were prepared and analyzed in triplicate on three consecutive days for muscle, and 1 day each for plasma, skin, and liver to combine the three series of the three days.

The statistical analysis of validation data was based on the accuracy profile using e. noval® software, Version 4.1 b (Pharmalex, Liège, Belgium). The concentrations of the validation samples were calculated from the experimental result to determine mean relative bias, repeatability, intermediate precision, and β-expectation tolerance interval limits with a 90% level. The acceptance limit was set at ± 50%.

2.6. Pharmacokinetic analysis

For the dosing during treatment and depuration periods, concentrations under the lower limit of quantification (LOQ) were discarded. Samples above the upper LOQ were diluted to enter into the validated range. Matrix-matched calibration curves were performed for the dosing of VPBO in several batches. The equation of the curves from VPBO dosing were used to assess the concentration of DLVPBO, assuming the mass spectrometric response would be equivalent, because no specific analytical standard is commercially available for this metabolite.

A non-compartmental model was used to determine the pharmacokinetic parameters. All pharmacokinetic analyses were

performed with Phoenix WinNonlin 8.2 software (Certara, Saint Louis, MO, USA).

2.6.1. Non-compartmental analysis

The observed data were sparse; one point per animal and six animals per time point were used. In this type of design, it was not possible to distinguish inter-individual from intra-individual variability, and consequently the present analysis focused on mean parameters and not on inter-individual variability. Therefore, it was only possible to calculate the standard error of the mean (SEM) for two parameters C_{max} and AUC_{last}.

The maximum concentration (C_{max}) and the time to reach it (T_{max}) were estimated from each tissue concentration versus the time profile.

For plasma or tissues, the total area under the time curve (AUC_{inf}) was determined using the linear trapezoidal rule with extrapolation to infinity. Extrapolation $AUC_{(Clast\ inf)}$ was based on the following equation:

$$AUC_{(Clast-inf)} = \frac{C_{last}}{\lambda_z}$$

where C_{last} is the last observed concentration and λ_z the slope of the terminal phase.

Consequently, the AUC_{inf} was calculated by:

$$AUC_{inf} = AUC_{(0-Clast)} + AUC_{(Clast-inf)}$$

where $AUC_{(0\ Clast)}$ is the AUC between 0 and C_{last}.

The terminal slope was estimated from the linear part of the terminal phase by at least three points, and was conserved if the coefficient of determination r^2 was >0.95.

The half-life of compounds ($t_{1/2}\ \lambda_z$) was determined using λ_z by the following formula:

$$t_{1/2\ \lambda_z} = \frac{0.693}{\lambda_z}$$

Partial areas were also estimated by linear trapezoidal method between [0-1d], [1-5d], [5-17d], and [17d-65d] i.e. the treatment period, the first depuration period, the second period and the last period after the treatment respectively.

The mean residence time (MRT) was calculated using the linear trapezoidal rule between 0 and C_{last} or with extrapolation to infinity. Apparent total body clearance ($Cl_{tot/F}$) and apparent volume of distribution at steady state (Vss/F) were also determined by:

$$CL_{tot/F} = \frac{Dose}{AUC_{inf}}$$

and. $Vss/_F = MRT\ x\ CL_{ss}$

For both the parent compound and its major metabolite, the time to reach the concentration at the LOQ was not measured. However, it was estimated by extrapolation using a simple exponential equation defined by the elimination rate and the apparent volume of distribution.

$$C = A \times e^{-\lambda_z \times t}$$

Where C is the tissue concentration, λ_z is the elimination rate and A is the fitted apparent constant.

2.6.2. Statistical analysis

Pharmacokinetic parameters (AUC_{last}, C_{max}) are expressed as arithmetic means, with associated standard error of the mean. The NCA sparse methodology calculates pharmacokinetics parameters based on the mean profile for all the individuals in the dataset. The NCA object calculates the standard error for the mean concentration curve's maximum value (Cmax), and for the area under the mean concentration curve from dose time through the final observed time. These parameters obtained in muscle and skin for VBPO and DLVBPO were compared by a *t*-test. A level a significance of 5% was retained.

3. Results

3.1. Analytical method performance for VPBO analysis

Linear regression with 1/X weighting was selected as the regression model for the validation in muscle on three different days, yielding the best response function and the best accuracy profile among those tested. Quadratic regression with 1/X weighting was selected as the regression model for global validation in plasma, skin, and liver matrices. The global validation was performed on three days, with one day of validation for each matrix (Hubert et al., 2004, 2007a, 2007b). The corresponding results are presented in Supplementary Table S1.

Trueness was lower than 10% in recovery on the validation range from 0.5 to 50 μg kg ^{1} (or μg.L ^{1} for plasma), except at 0.5 μg kg ^{1} (or μg.L ^{1} for plasma) for the three combined matrices for which recovery was 112.3%. This value obtained for three matrices that were entirely different and at low concentrations, was however, considered satisfactory. For precision (repeatability and intermediate precision), relative standard deviations (RSDs) did not exceed 10% for muscle from 0.5 to 50 μg kg ^{1}. At 0.5 μg kg ^{1} (or μg.L ^{1}: plasma), RSDs did not exceed 15% for the combined plasma-skin-liver matrices.

The β-expectation tolerance interval limits (%) were within the acceptance limits (±50%) for both muscle and combined plasma-skin-liver matrices. This method is thus accurate from 0.5 to 50 μg kg ^{1} (or μg.L ^{1} for plasma) for all matrices.

The limit of detection (LOD) was estimated at 0.15 μg kg ^{1} (or μg.L ^{1} for plasma) for all matrices. The estimated lower and upper LOQs were 0.5 and 50 μg kg ^{1} (or μg.L ^{1} for plasma). For muscle, the risk of error was below 0.1%. For the combined plasma-skin-liver matrices from 0.5 to 50 μg kg ^{1} (or μg.L ^{1} for plasma), this risk was below 2%.

For muscle, the relative uncertainty was limited to 20%, and for the combined plasma-skin-liver matrices, it was limited to 17%, except at 0.5 μg kg ^{1} (L ^{1} for plasma) (31%) (Supplementary Table S2).

The equations for the linearity of the results are provided in Supplementary Table S3. The coefficients of determination R^2 were above 0.99. The β-expectation tolerance interval limits were within the acceptance limits (±50%) for all matrices, regardless of the concentration of the validation standards, as shown in Supplementary Figure S1.

3.2. Metabolites of VPBO

Metabolites were detected from the total ion current of chromatograms in muscle, plasma, skin, and liver by MetWorks software, and metabolites were then tentatively identified based on their accurate masses, mass errors, and retention times compared to VPBO retention times. As shown in Table 1, there were 15 metabolites of VPBO in total found in rainbow trout. The exact and measured masses matched with a mass error below 5 ppm, providing support for the proposed elemental compositions of metabolites. During the treatment period, the total amount of metabolites followed the order: liver > muscle ≅ plasma > skin. Otherwise, during the depuration period, the total amount of

Table 1
In vivo LC-Orbitrap-HRMS data for VPBO and its metabolites in rainbow trout. Metabolites M7, M9, M12, and M13 were not detected contrary to our previous *in vitro* study (ND: non detected).

Compound ID	Reaction proposed	Δm/z	Molecular formula	Calculated mass	Measured mass	Error (ppm)	RT (min)
M0 (VPBO)	/	/	$C_{33}H_{40}N_2$	478,3216	478,3205	2,3	7,1
M1	N-deethylation	−28,0313	$C_{31}H_{36}N_2$	450,2903	450,2895	1,77	6,5
M2	double N-deethylation	−56,0626	$C_{29}H_{32}N_2$	422,259	422,2583	1,65	6,0
M3	triple N-deethylation	−84,0939	$C_{27}H_{28}N_2$	394,2277	394,227	1,77	5,4
M4	quadruple N-deethylation	−112,1252	$C_{25}H_{24}N_2$	366,1964	366,1958	1,64	5,0
M5	quintuple N-deethylation	−140,1565	$C_{23}H_{20}N_2$	338,1651	338,1646	1,48	4,7
M6	N-demethylation	−14,0157	$C_{32}H_{38}N_2$	464,3059	464,305	1,94	6,8
M7	N-deethylation + N-demethylation	−42.0470	$C_{30}H_{34}N_2$	436.2746	ND	ND	ND
M8	N-oxidation	15,9949	$C_{33}H_{40}N_2O$	494,3165	494,3158	1,41	6,0
M9	N-deethylation + N-oxidation	−12.0364	$C_{31}H_{36}N_2O$	466.2852	ND	ND	ND
M10	N-oxidation + double N-deethylation	−40,0677	$C_{29}H_{32}N_2O$	438,2539	438,2538	0,23	5,5
M11	N-oxidation + triple N-deethylation	−68,0990	$C_{27}H_{28}N_2O$	410,2226	410,2221	1,21	5,2
M12	N-oxidation + deshydrogenation	13.9792	$C_{33}H_{38}N_2O$	492.3008	ND	ND	ND
M13	N-deethylation + N-oxidation + deshydrogenation	−14.0521	$C_{31}H_{34}N_2O$	464.2695	ND	ND	ND
M14	N-oxidation + deshydrogenation + double N-deethylation	−42,0833	$C_{29}H_{30}N_2O$	436,2382	436,2377	0,06	5,1
M15	N-oxidation + deshydrogenation + triple N-deethylation	−70,1146	$C_{27}H_{26}N_2O$	408,2069	408,2063	1,47	4,8
M16	double-bound reduction + N-deethylation	−26,0157	$C_{31}H_{38}N_2$	452,3060	452,3053	1,54	10,1
M17	double-bound reduction	2,0156	$C_{33}H_{42}N_2$	480,3373	480,3371	0,42	9,3
M18	double-bound reduction + double N-deethylation	−54,0470	$C_{29}H_{34}N_2$	424,2747	424,2739	1,89	8,5
M19	glucuronidation + N-oxidation	192,0270	$C_{39}H_{48}N_2O_7$	670,3486	670,3476	1,49	5,3

metabolites followed this order: muscle > skin ≈ liver > plasma. The intensities of signals for metabolites are shown in Supplementary Figure S2. The metabolites found in this animal experiment were quite similar to those found in a previous *in vitro* study (Dubreil et al., 2020b). However, we observed a few differences that are described below.

3.3. Phase I metabolites

The $[M]^+$ ions of metabolites M1 to M6 matched with dealkylation reactions regarding loss of masses of VPBO. The same dealkylated metabolites were observed as those in the *in vitro* study except that the deethylation + demethylation could not be observed *in vivo*. VPBO underwent successive deethylation for M1 to M5 (removal of 28.03130 Da) and demethylation for M6 (removal of 14.01565 Da). M1 (*m/z* 450.2903) to M5 (*m/z* 338.1651) had retention times of 6.5, 6.0, 5.4, 5.0, and 4.7 min, respectively. Retention times decreased with the number of deethylations, so the shortest retention time was assigned to quintuple N-deethylation (M5), consolidating the proposed pathway of successive deethylations. Metabolite M6 had a retention time of 6.8 and showed $[M]^+$ ion at *m/z* 464.3059.

Metabolites M8, M10, M11, M14, and M15 followed N-oxidation and also dehydrogenation for M14 and M15, as cited in the previous *in vitro* study (Dubreil et al., 2020b). However, metabolites M7 (deethylation + demethylation), M9 (deethylation + oxidation), M12 (oxidation + dehydrogenation), and M13 (deethylation + oxidation + dehydrogenation) detected in the *in vitro* study were not observed *in vivo*. M8, M10, M11, M14, and M15 eluted at 6.0, 5.5, 5.2, 5.1, and 4.8 min, respectively. Certain ions were observed at 16 Da higher compared to the non-oxidized ion, for example M9 (deethylation + oxidation) compared to M1 (deethylation).

The double-bound reduction reaction was observed more strongly in treated rainbow trout than after *in vitro* incubations for which the major metabolite identified was the deethyl-VPBO (M1) without the double-bound reduction. Three proposed reactions were observed, (1) the double-bound reduction reaction which is also very well described for triarylmethane dyes, (2) the double-bound reduction + deethylation reaction, and (3) the double-bound reduction + double deethylation reaction. Only metabolite M16 corresponding to reaction (3) was observed weakly during the previous *in vitro* incubation. Metabolite M17 could be proposed as the leuco form of VPBO at *m/z* 480.3371 and eluted at 9.3 min. It was at least 10 times less intense than M16 in muscle and skin (Table 2). M18 was observed between 1.1 and 3.3 times more intense than M17 in muscle and skin, corresponding to double-bound reduction + deethylation at *m/z* 424.2747 and retention time at 8.5 min. M16 was observed at least 10 times more intense in muscle and skin compared to M17 and M18, which could explain why it was the only ion detected *in vitro* that undergoes double-bound reduction. M16 was detected at *m/z* 452.3053 and retention time at 10.1 min. The chromatograms of M16 and the parent VPBO are shown in Fig. 1.

This *in vivo* metabolism study identified the most intense metabolite as M16 during the depuration period, as shown in the mean peak areas of metabolites in Supplementary Figure S2. This deethyl-leuco metabolite was found in the four matrices, and was also present in large amounts during the depuration period. Its identity was confirmed by the CID fragment ions (*m/z* = 423.18, 379.39, 303.38, 252.37) and compared to the fragmentation of the deethyl-VPBO carried out during a previous *in vitro* study. However, only one isomer could be retrieved *in vivo* compared to *in vitro* where two isomers where detected (Dubreil et al., 2020b). As a result, the deethyl-leuco VPBO (DLVPBO) was integrated in further data analysis to compare its pharmacokinetic parameters with those of VPBO.

3.4. Phase II metabolite

A single ion M18 detected at *m/z* 670.3486 was found probably to be a glucuronide metabolite with supplementary oxidation, corresponding to the difference in mass of *m/z* 192.0270 with VPBO. This ion was only detected in liver during the treatment and depuration periods. The error on the measured mass was 1.49 ppm, which is low. Moreover, the retention time was 5.3 min, indicating that this ion eluted earlier than VPBO. The retention time of M18 supported the assumption of its identification as a glucuronide. In fact, glucuronide metabolites are classified as phase II metabolites and as a rule, offer weaker retention because of the high polarity of

Table 2
Peak area ratios between main metabolites of VPBO detected in muscle, liver, plasma and skin during treatment and during depuration.

Peak area ratios between main metabolites of VPBO	Treatment				Depuration			
	muscle	liver	plasma	skin	muscle	Liver	plasma	skin
M16/M1	11	1	24	4	63	6	273	21
M16/M17	57	356	17	33	16	25	9	29
M16/M18	23	12	105	10	15	5	28	11
M18/M17	2.5	30.2	0.2	3.3	1.1	5.2	0.2	2.6

the glucuronide part.

3.5. Comparative pharmacokinetic analysis of VPBO and major metabolite DLVPBO in rainbow trout

3.5.1. Uptake and depuration of VPBO in different tissues

Water bath exposure of rainbow trout in a tank containing 0.1 mg.L ^{1} of VPBO for one day did not lead to deaths. VPBO was well tolerated by the exposed rainbow trout. At each time point, matrices (muscle, plasma, skin, and liver) were sampled carefully to carry out the analysis of residues of VPBO in each matrix by the validated LC-HRMS method. The mean concentrations of VPBO (±SD, standard deviation) in muscle, plasma, skin, and liver are shown in Table 3.

During the uptake period, the mean VPBO concentrations in muscle and skin increased until the last sampling time point at 24 h (T4) and were measured at 99.9 µg kg ^{1} ±54.4 for muscle, and 263 µg kg ^{1} ±78.2 for skin. Unlike this increase, the highest concentrations for plasma and liver occurred at the first date of sampling at 2 h (T1) after the beginning of treatment. The concentrations were 567 µg.L ^{1} ±300 for plasma and 1846 µg kg ^{1} ±517 for liver. These levels decreased subsequently during the uptake period. At the end of the uptake period after 24 h, the highest concentration levels in matrices followed this order: liver > skin > muscle > plasma. The plasma concentrations decreased rapidly during this period from 567 µg.L ^{1} ±300 at T1 to 9.27 µg.L ^{1} ±7.35 at T4 (Supplementary Figure S3).

After placing the rainbow trout in a clean water bath for depuration, the concentrations in the tissues and plasma decreased gradually over the 64 days of depuration. At the end of this period, concentrations were still above the LOQ for muscle, skin and liver. VPBO was barely detectable in plasma, with concentrations below the LOQ at 5 days (T7) after withdrawal of treatment. The levels reached in muscle and skin were comparable after 33 days and were measured at 2.26 µg kg ^{1} ±0.48 for muscle and 2.85 µg kg ^{1} ±1.99 for skin at the end of the depuration period.

3.5.2. Pharmacokinetic analysis of VPBO and DLVPBO

Pharmacokinetic parameters were determined using sparse sampling non-compartmental analysis and are presented in Table 4 for VPBO in plasma and tissues and for DLVPBO in only muscle and skin, because it is edible tissue, and based on the calibration model of VPBO since no standard product is available for DLVPBO.

3.6. Parent VPBO

The maximum plasma concentration C_{max} (567 ± 301 µg.L ^{1}) after water bath treatment was reached at time T_{max} of 0.083 d (2 h) for VPBO, demonstrating rapid absorption. The apparent total body clearance (Cl_{tot}/F) was 0.34 L kg ^{1}. d ^{1} for plasma. The apparent volume of distribution at steady state (Vss/F) was 0.095 L kg ^{1}. The elimination half-life ($t_{1/2}$ λ_z) in plasma was short, (0.73 day) compared to other tissues. The area under the curve, AUC_{inf}, was calculated as 116 µg d.L ^{1}. The initial distribution of VPBO in tissues showed the highest concentration C_{max} in liver at 1847 µg kg ^{1} ± 211, at 99.9 µg kg ^{1} ± 22.2 in muscle, and at 264 µg kg ^{1} ± 35.9 in skin, occurring at T_{max} of 0.083 days (2 h) for liver, and at 1 d for muscle and 2 d for skin. AUC_{inf} in skin estimated at 2781 µg d.kg ^{1} was 2 and 2.75 times higher than in liver and muscle, respectively. The mean residence time (MRT_{inf}) was longer in skin and muscle, with values of 12.7 and 20.7 days respectively, compared to liver (5 days). The terminal elimination phase was the longest in muscle with a $t_{1/2}$ λ_z estimated at 17.1 days.

3.7. Main metabolite: DLVPBO

For the main metabolite identified, DLVPBO, the parameters were assessed only in muscle and skin (Table 4). The different pharmacokinetic profiles between the parent VPBO and the major metabolite DLVPBO are plotted in Fig. 2. The C_{max} values were lower for DLVPBO estimated at 31 µg kg ^{1} ± 3.8 in muscle and 70.6 µg kg ^{1} ± 9.0 in skin. A lower elimination rate of DLVPBO, and consequently a terminal elimination phase, was observed in muscle (22.5 days) compared to the elimination rate of VPBO (17.1 days). The mean residence time (MRT_{inf}) was estimated to be 43.1 days in muscle and 29.9 days in skin for DLVPBO, versus 20.7 days and 12.7 days for VPBO respectively. The computations of partial areas of VPBO and DLVPBO for different sampling times in skin showed systematically higher concentrations of parent compound compared to DLVBPO, in all period. However, in muscle, higher concentrations of DLVPBO were recovered after 17 days. (Fig. 3).

4. Discussion

This study assessed for the first time the metabolism, pharmacokinetics and tissue residues in rainbow trout exposed to VPBO dye in a water bath. During a preliminary test (data not shown), high toxicity of VPBO was observed for a dose at 0.8 mg.L ^{1}. Different concentrations of malachite green MG in bath treatment for aquaculture are depicted in the literature. The concern is always about the potential for human toxicity in the presence of malachite and leucomalachite green in fish tissues. Alderman and Clifton-Hadley (1993) exposed rainbow trout to 1.6 mg.L ^{1} of MG for 40 min, at two different temperatures. Máchová et al. (1996) applied treatment of rainbow trout at 0.2 mg.L ^{1} of MG for 6 days in a water bath. Bajc et al. (2011) chose to apply different doses ranging from 1 mg.L ^{1} to 1.5 mg.L ^{1} of waterborne MG for different exposure times (1 h or 3 h). These studies could only provide a guide for waterborne treatment of rainbow trout by triarylmethane-like dyes because no data could be retrieved for the administration of VPBO in aquaculture. However, in our previous metabolomics study, a dose of 0.05 mg.L ^{1} for rainbow trout exposed to VPBO for two days was applied following the experimental design by Dubreil et al. (2019b). The number of metabolites found in the metabolomics study was quite low (5 metabolites) compared to all those found in the *in vitro* study (15 metabolites). So a higher concentration was tested at 0.1 mg/L demonstrating notoxicity for the fish (Dubreil et al., 2019a, 2020b). The final dose

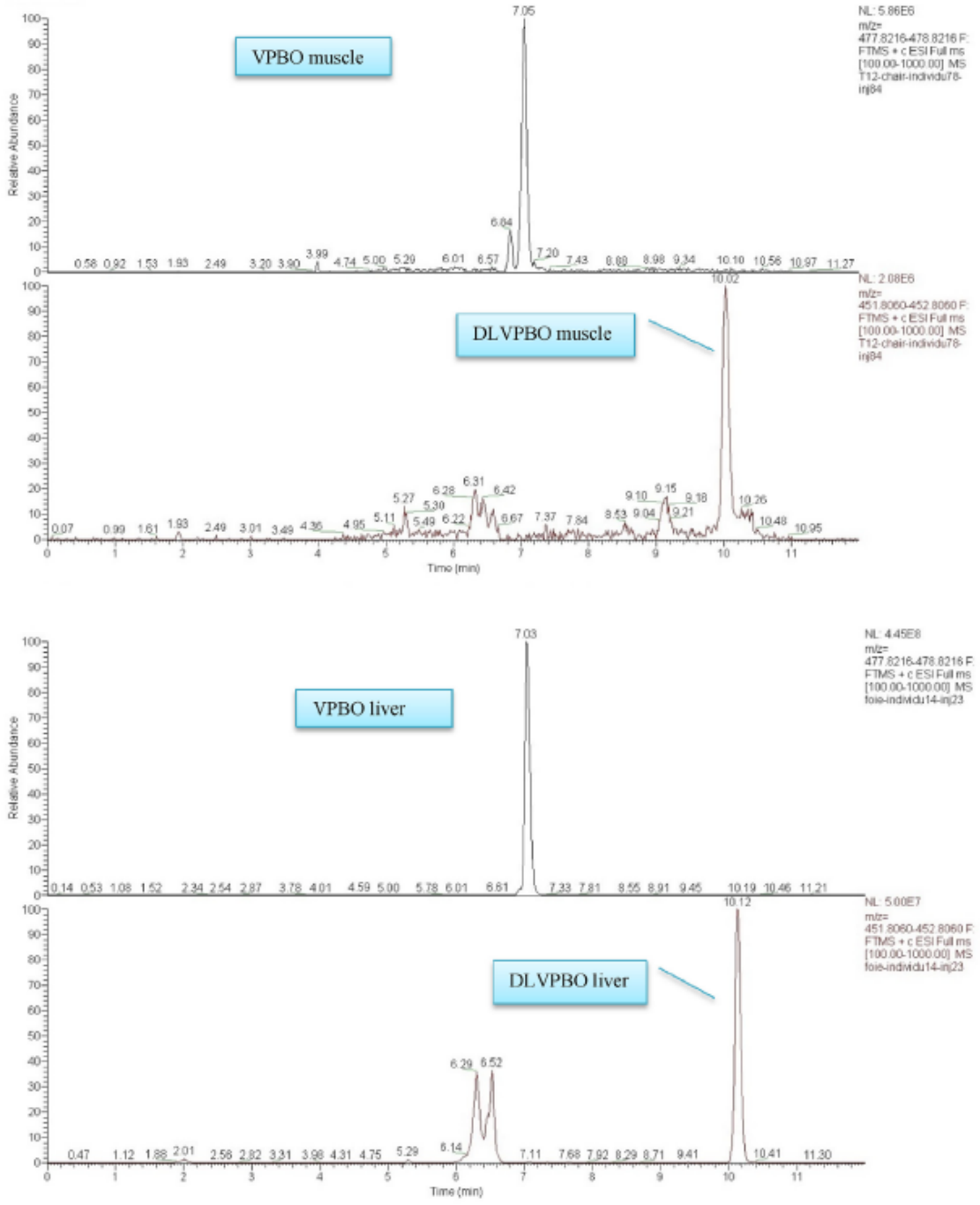

Fig. 1. Chromatogram of VPBO and principal metabolite M16 deethyl-leuco-VPBO (DLVPBO) in muscle (at T12), liver (at T14), skin (at T5), and plasma (at T3).

of 0.1 mg.L ^{1} of VPBO diluted in a water bath for one day was selected.

The first step in this study was to examine the metabolites obtained and potentially the main relevant metabolite, that could be even more persistent than the parent compound VPBO. The determination of a persistent metabolite as a marker residue is important to track administration of a treatment over time after fish exposure to the prohibited substance. In addition, this marker

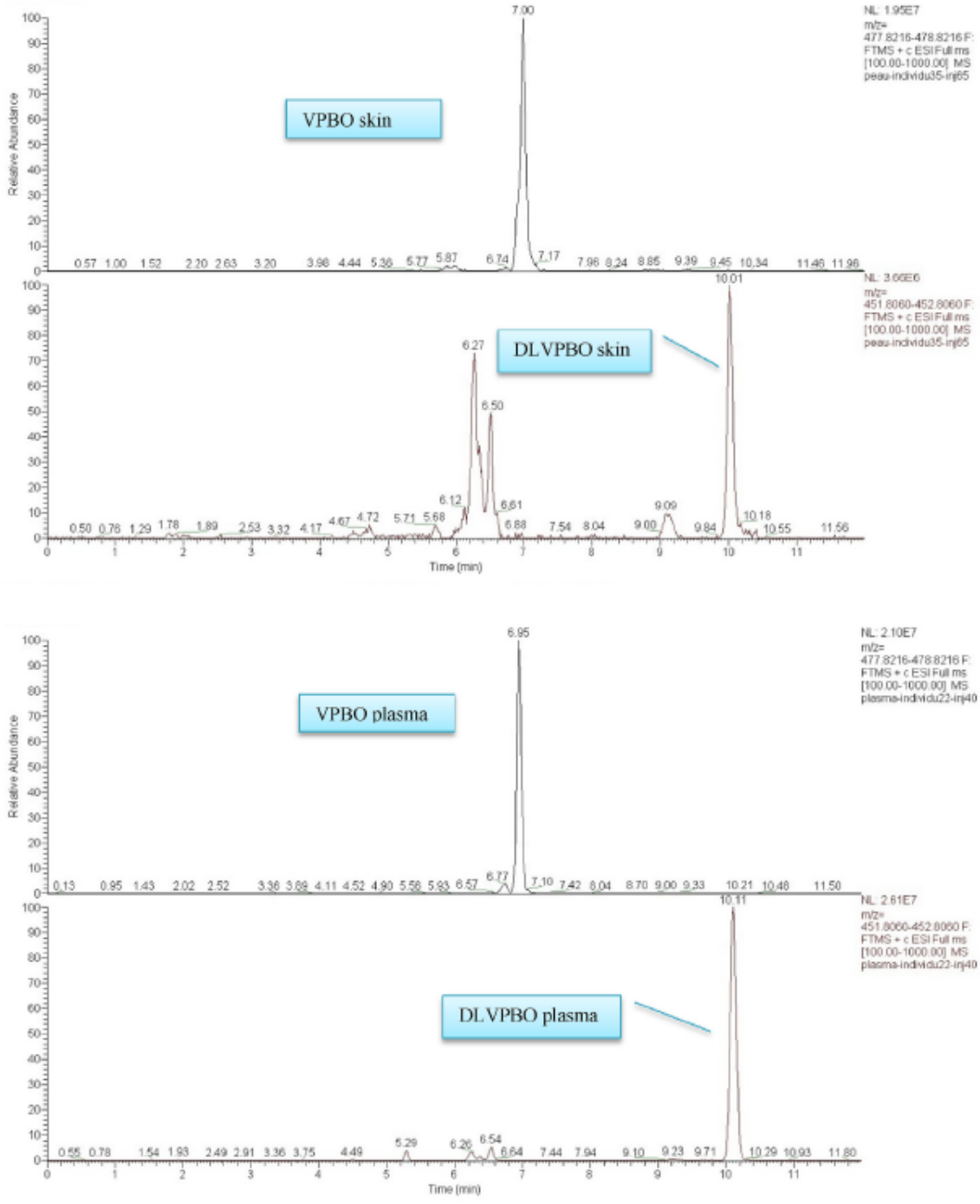

Fig. 1. (*continued*).

residue can be more toxic than the parent compound. Tacal and Özer (2007) found that the generation of triarylmethane metabolites did not alter the toxic load on exposed organisms because metabolites were at least as toxic as the parent compounds. Our *in vitro* metabolite investigation demonstrated that VPBO is biotransformed into 15 metabolites in the different biological tissues of rainbow trout, with in particular a greater amount of metabolites detected in liver (Dubreil et al., 2020b). During the treatment period in this study, the total amount of metabolites (expressed in peak area) followed this order: liver > skin ≅ plasma > muscle, whereas during the depuration period, the total amount of metabolites followed this order: liver > skin ≅ muscle > plasma. This estimated metabolic rate was in line with the rapid depuration by the liver found for other triarylmethane dyes with a similar

Table 3
Concentrations of VPBO in muscle, plasma, skin, and liver of rainbow trout after exposure to VPBO (n = 6 trout) at a dose of 40 mg.kg^{-1} b.w.

Date of treatment		Muscle µg.kg^{-1} (mean ± SD)	Plasma µg.L^{-1} (mean ± SD)	Skin µg.kg^{-1} (mean ± SD)	Liver µg.kg^{-1} (mean ± SD)
Uptake period (in days)					
T0	0	0	0	0	0
T1	0.083 d (2 h)	60.50 ± 13.34	566.64 ± 300.54	83.01 ± 27.26	1846.08 ± 517.26
T2	0.208 d (6 h)	77.86 ± 20.68	138.03 ± 101.29	174.98 ± 35.92	1468.48 ± 687.17
T3	0.417 d (10 h)	75.30 ± 39.94	32.15 ± 21.38	162.02 ± 49.08	825.21 ± 674.09
T4	1 d (24 h)	99.91 ± 54.43	9.27 ± 7.35	263.54 ± 78.17	300.32 ± 131.21
Depuration period (in days)					
T5	2 d	88.51 ± 44.72	1.83 ± 2.35	263.95 ± 88.03	67.29 ± 30.78
T6	3 d	38.39 ± 19.49	0.51 ± 0.37	219.05 ± 110.80	56.95 ± 44.93
T7	5 d	42.08 ± 13.82	<LOQ	115.68 ± 39.65	17.77 ± 8.41
T8	9 d	16.89 ± 7.79	<LOD	80.54 ± 45.34	8.67 ± 3.96
T9	17 d	16.01 ± 6.56	<LOQ	56.94 ± 29.82	3.24 ± 1.58
T10	34 d	8.52 ± 2.03	<LOQ	9.05 ± 5.22	2.17 ± 1.00
T11	49 d	6.02 ± 2.73	<LOD	6.42 ± 2.54	2.89 ± 3.30
T12	65 d	2.26 ± 0.48	<LOD	2.85 ± 1.99	0.60 ± 0.39

Table 4
Pharmacokinetic parameters of VPBO determined by sparse sampling non-compartmental analysis in rainbow trout tissue and plasma, and of metabolite DLVPBO in muscle and skin after a water bath of rainbow trout in a bath containing 40 mg.kg^{-1} b.w. Of VBPO for 24 h.

	Parent VPBO				DLVPBO	
	liver	plasma	muscle	skin	muscle	skin
λ_z (d^{-1})	0.0443	0.9451	0.0406	0.0634	0.0310	0.0384
$T_{1/2}$ λ_z (d)	15.6	0.73	17.1	10.9	22.5	18.1
AUC_{last} (µg.d.L^{-1} or kg^{-1}) ±SEM	1406 ± 130	116 ± 17	955 ± 57$^{(a)}$	2736 ± 219$^{(a)}$	945 ± 64$^{(a)}$	2528 ± 143$^{(a)}$
AUC_{inf} (µg.d.L^{-1} or kg^{-1})	1420	116	1010	2781	1175	2780
AUC_{extrap} (%)	0.96	0.17	5.52	1.62	19.53	9.72
Cl_{tot}/F (L.kg^{-1}.d^{-1})	0.0281	0.34	0.0396	0.0144	0.0334	0.0143
MRT_{inf} (d)	5.03	0.28	20.7	12.7	43.1	29.9
Vss/F (L.kg^{-1})	0.142	0.095	0.819	0.183	1.46	0.430
T_{max} (d)	0.083	0.083	1.00	2.00	2.00	17.0
C_{max} (µg.L^{-1} or kg^{-1}) ±SEM	1847 ± 211	567 ± 123	99.9 ± 22.2$^{(b)}$	264 ± 35.9$^{(b)}$	31.0 ± 3.8$^{(b)}$	70.6 ± 9.0$^{(b)}$

λ_z first order rate constant associated with the terminal portion of the curve; $T_{1/2}$ λ_z: terminal half-life; AUC_{last}: area under the curve (AUC) from time of dosing (0) to the time of the last quantifiable concentration (i.e. above LOQ); AUC_{inf}: AUC extrapolated from time of dosing (0) to infinity; AUC_{extrap}: percentage of AUC_{inf} that is due to extrapolation from T_{last} to infinity; Cl: clearance; MRT_{inf}: MRT extrapolated to infinity using the last quantifiable concentration for extrapolation; Cl_{tot}/F: total body clearance; Vss/F: volume of distribution at steady state; T_{max}: time of maximum tissue or plasma concentrations; C_{max}: maximum tissue or plasma concentrations. Standard error of the mean (SEM) was estimated for C_{max} and AUC_{last}. (a): not statistically significantly different ($p > 0.05$) between VBPO and DLVBPO. (b): statistically significantly different ($p \leq 0.05$) between VBPO and DLVBPO.

structure (Plakas et al., 1996; Decroos et al., 2009). Furthermore, high levels of total MG residues in the liver of channel catfish (*Ictalurus punctatus*) for two weeks after waterborne exposure to a C^{14}-MG solution were reported by Plakas et al. (1996). In addition, the liver, along with the gills, is an organ of major importance in the ecotoxicology of fish due to its high metabolic capacities and its crucial role in detoxification (Gomez et al., 2010). In this study, VPBO was metabolized particularlyinto M16, M15 and M17 in muscle, plasma and skin during the depuration period, as well as into M16 and M17 in the liver. These metabolites correspond to *m/z* 452,3060 (M16, proposed as N-deethyl-leuco VPBO or DLVPBO), *m/z* 408.2069 (M15, proposed as N-oxidated dehydrogenated triple N-deethyl VPBO), and *m/z* 480,3373 (M17, proposed as leuco-VPBO). The metabolites found (the main metabolite and the others identified), suggest that dealkylation (deethylation) and double-bound reduction are major metabolic pathways. The M16 was also found in our previous metabolomics study (Dubreil et al., 2019b), ranking first in muscle, and third in the liver. In the same metabolomics study, the M17 was also detected, ranking first in the liver, but not detected in muscle, whereas it was detected in high amounts in the present study in muscle. Similar pathways of dealkylation and oxidation for MG were described by Doerge et al. (1998), showing that levels of leucoMG in edible tissues of fish exceeded those of MG, and consequently confirmed that leuco-MG was a relevant residue marker for regulatory determination of MG misuse. In this study on VPBO, a substance derived from a triarylmethane structure similar to MG, we found that the metabolite leading to the highest signal intensity in all biological matrices was M16, proposed as DLVPBO.

The assessment of pharmacokinetic parameters was first carried out for the parent compound. During the uptake period, the concentration of VPBO in plasma and liver increased rapidly, and concentrations were the highest at the beginning of the treatment, suggesting efficient uptake by the gills, and to a lesser degree by skin then muscle. The role of the gills in the uptake of MG, a similar triarylmethane dye, was described for the first time by Poe and Wilson (1983). The high concentration of VPBO in liver was directly associated to the role of liver, where hepatic biotransformation directly relates to bioaccumulation of lipophilic contaminants in fresh water fish (Schultz et al., 1999). Moreover, an increase in concentrations was observed at the end of the uptake period for muscle and skin, probably due to reabsorption of VPBO via excrements eliminated in the closed water bath. To the best of our knowledge, no data are available on the level of VPBO after treatment in fish for comparison. During our study, a rapid decline of VPBO was observed in plasma. The elimination half-life was calculated as 0.73 days (around 18 h) in plasma. For Alderman and Clifton-Hadley (1993) determined $t_{1/2}$ λ_z of trout plasma to be 0.62 days at 8 °C, and 14.5 days at 16 °C, so a longer elimination rate with the increasing of temperature. In the present study, rainbow trout

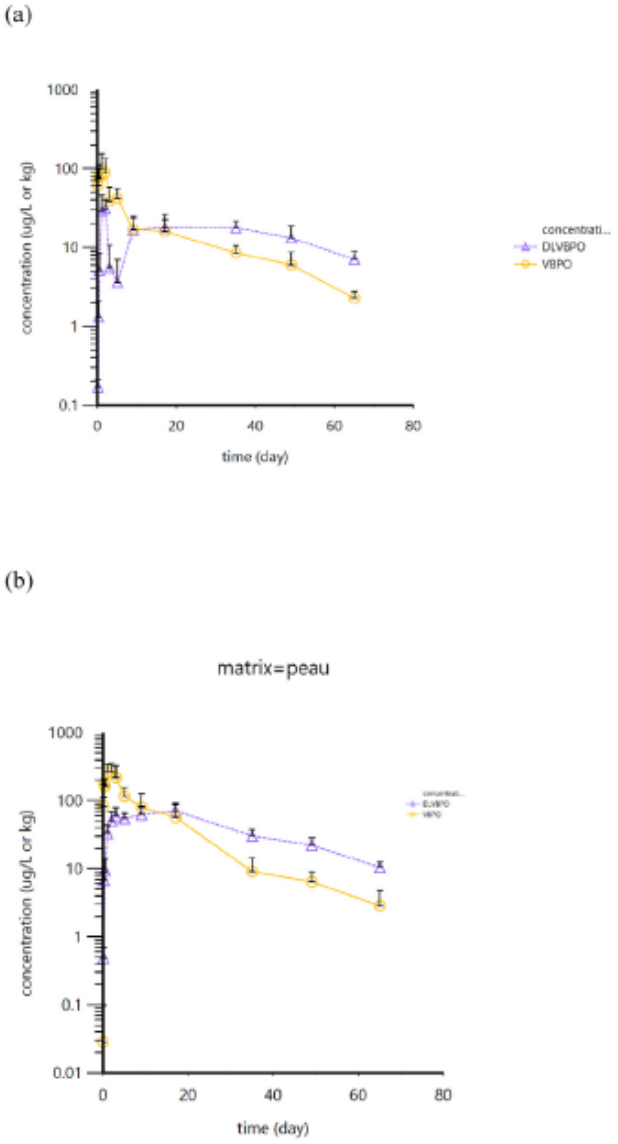

Fig. 2. Concentration profile of VPBO and DLVPBO in rainbow trout muscle (a) and skin (b) after water bath with VBPO at a dose of 40 mg.kg^{-1} b. w.

were kept at 13 °C in a water bath, and temperature has been described elsewhere as a key factor for the elimination of MG as well as other environmental factors (Lanzing, 1965). VPBO tends to be eliminated faster than MG around the same temperature, presumably because it is bio-transformed into a broader panel of metabolites. In tissues, the decrease in VPBO concentrations was slower than in plasma. Our results show that the mean residence time of VPBO in muscle and skin, was higher than in liver and plasma.

For the major metabolite identified, DLVPBO, the amount of metabolite (in peak area) was converted in concentration considering the same analytical response than the parent VPBO; the concentrations were assessed only for muscle and skin in order to estimate pharmacokinetic parameters for DLVPBO in the edible matrix that need a definition of residue marker. The estimated C_{max} values in muscle and skin were three and eight times lower than those of the parent compound, respectively but mean residence times were higher for the metabolite. In fact, LVPBO tend to decrease more slowly than its parent molecule taking into account the biologic variability. The elimination half-life in muscle and skin was slightly higher compared to VPBO, which confirmed the same fate of DLVPBO as the main metabolite of MG (LMG). In fact, Plakas et al. (1996) demonstrated that MG and LMG half-lives in catfish muscle were 2.8 and 10 days, respectively. MG and LMG were also more persistent in muscle than in plasma, with a major role of metabolism in the clearance of the parent compound. The difference in elimination rates between the parent compound MG and its metabolite residue marker LMG seems more pronounced than for VPBO and DLVPBO. This could be due to lipid content because in the Plakas et al. (1996) study, the model was evaluated for catfish, which is a fattier fish species than rainbow trout, and LMG accumulates in fat. In addition, MG is less lipophilic than VPBO (log P (MG) = 0.62 and estimated log P (VPBO) = 4.06). Fat content has actually been proven to act on metabolite levels. In a study on carp and trout, Jiang et al. (2009) found that there was a difference between three common freshwater fish, *Parabramispekinensis* (plant-eating fish), *Carassiusauratus* (omnivorous fish) and *Ophiocephalusargus* (carnivorous fish), with LMG levels significantly correlated with lipid content in fish tissue. In our study, the rainbow trout were not very fatty, weighing a mean of 117 g at the start and 232 g at the end of the experiment. As a result, differences could be found for the depuration rates of VPBO and DLVPBO in other fatty fish.

The time needed for the metabolite DLVPBO concentration to decrease below to the LOQ (LOQ = 0.5 µg kg ^{1}) was 149 days in edible muscle tissue, whereas it appears to be shorter for VPBO (110 days). It may be beneficial to investigate this tendency in other fish species. Our results, showing longer persistence of the DLVPBO metabolite in muscle and especially in skin, compared to parent VPBO, are of particular interest. The concentrations found in the skin highlighted that monitoring of VPBO for food safety or environmental contamination should not dissociate the muscle from the skin. This study demonstrated that the bioaccumulation of VPBO and some metabolite residues in edible fish tissues is an important aspect for consumer's health regulatory agencies should be aware of. However, these results should be interpreted with caution to take into account the *in vivo* variability. It would be necessary to produce a toxicological assessment of DLVPBO in order to propose definitely the sum of VPBO and DLVPBO as the relevant residue marker of an illegal treatment by VPBO in farmed rainbow trout.

5. Conclusion

The results of the current study demonstrate that VPBO is rapidly absorbed and well distributed in rainbow trout muscle, skin, and liver, after water bath administration for one day. VPBO is then rapidly converted into 15 metabolites, with one metabolite found to be more intense and persistent, proposed as deethyl-leuco-VPBO (DLVPBO). These results highlight the key role played by the liver in the metabolism of VPBO. A depuration period of 60 days enabled us to compare the pharmacokinetic profiles of VPBO and DLVPBO. The metabolic profiles showed that the parent drug VPBO occurs at higher concentrations in muscle and skin at the start of the uptake period, but its concentrations fall below those of DLVPBO in muscle after 17 days. At 60 days of depuration, the concentrations of VPBO in muscle and skin (mean of 2.5 µg kg ^{1}) are still slightly above the limit of quantification of 0.5 µg kg ^{1}, whereas concentrations of the DLVPBO metabolite were found to be a mean of 8.8 µg kg ^{1} in the same tissues. For these reasons, VPBO and its major metabolite DLVPBO, an appropriate residue marker,

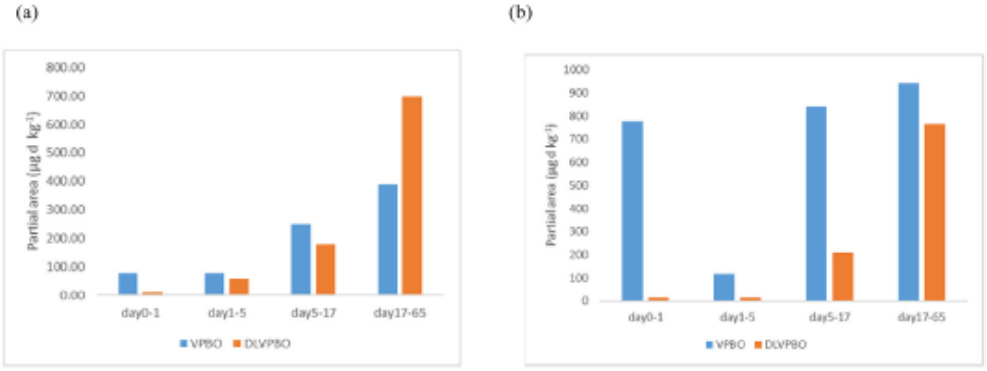

Fig. 3. Partial area (µg.day.kg^{-1}) of VPBO and DLVPBO for different time points in rainbow trout muscle (a) and skin (b).

should both be monitored without dissociating adhering skin, for effective residue control.

Author contribution statement

E.D. and E.V. conceived the study. E.V. supervised the project and supervised the findings of this work. P.S. and D. H–P. helped supervise the project. E.D. and M.L. developed the theory and performed the computations. D.H–P. encouraged E.D. to investigate the metabolism aspect and PS the pharmacokinetics aspect. E.D. and J-M.D. carried out the analytical experiment. J-M.D. carried out the sample preparation. J-M. D and E.D. verified the analytical methods. M.D. and T.M. carried out the animal experiment. E.D., M.D. and T.M. designed and planned the animal experiment and M.D. performed the experiments. M.L., A.V. and P.S. performed the pharmacokinetics computations. M.L., A.V., P.S. contributed to the interpretation of the results. E.D. wrote the manuscript with support from M.L., A.V. and E.V. All authors provided critical feedback and helped shape the research, analysis and manuscript.

Declaration of competing interest

The authors declare that they have no known competing financial interests or personal relationships that could have appeared to influence the work reported in this paper.

Acknowledgement

The authors thank the European Commission Directorate-General for Health and Food Safety (European contribution to the European Union Reference Laboratory SI2.726842 & SI2.777451), which enabled this work to be carried out.

Appendix A. Supplementary data

Supplementary data related to this article can be found at https://doi.org/10.1016/j.chemosphere.2020.127636.

References

Alderman, D.J., 1982. In vitro testing of fisheries chemotherapeutants. J. Fish. Dis. 5, 113–123.
Alderman, D.J., 1985. Malachite green: a review. J. Fish. Dis. 8, 289–298.
Alderman, D.J., Clifton-Hadley, R.S., 1993. Malachite green: a pharmacokinetic study in rainbow trout, Oncorhynchus mykiss (Walbaum). J. Fish. Dis. 16, 297–311.
Bajc, Z., Jenčič, V., Šinigoj Gačnik, K., 2011. Elimination of malachite green residues from meat of rainbow trout and carp after water-born exposure. Aquaculture 321, 13–16.
Bergwerff, A.A., Kuiper, R.V., Scherpenisse, P., 2004. Persistence of residues of malachite green in juvenile eels (Anguilla anguilla). Aquaculture 233, 55–63.
Culp, S.J., Blankenship, L.R., Kusewitt, D.F., Doerge, D.R., Mulligan, L.T., Beland, F.A., 1999. Toxicity and metabolism of malachite green and leucomalachite green during short-term feeding to Fischer 344 rats and B6C3F1 mice. Chem. Biol. Interact. 122, 153–170.
CVMP, 1998. Establishment of Maximum Residue Limits for Salmonidae and Other Fin Fish.
Decroos, C., Li, Y., Bertho, G., Frapart, Y., Mansuy, D., Boucher, J.L., 2009. Oxidative and reductive metabolism of tris(p-carboxyltetrathiaaryl)methyl radicals by liver microsomes. Chem. Res. Toxicol. 22, 1342–1350.
Dervilly-Pinel, G., Chereau, S., Cesbron, N., Monteau, F., Le Bizec, B., 2015. LC-HRMS based metabolomics screening model to detect various β-agonists treatments in bovines. Metabolomics 11, 403–411.
Doerge, D.R., Churchwell, M.I., Gehring, T.A., Pu, Y.M., Plakas, S.M., 1998. Analysis of malachite green and metabolites in fish using liquid chromatography atmospheric pressure chemical ionization mass spectrometry. Rapid Commun. Mass Spectrom. 12, 1625–1634.
Dubreil, E., Mompelat, S., Kromer, V., Guitton, Y., Danion, M., Morin, T., Hurtaud-Pessel, D., Verdon, E., 2020a. Corrigendum to "Dye residues in aquaculture products: targeted and metabolomics mass spectrometric approaches to track their abuse [Food Chem. 294 (2019) 355–367]. Food Chem. 306, 125539.
Dubreil, E., Mompelat, S., Kromer, V., Guitton, Y., Danion, M., Morin, T., Hurtaud-Pessel, D., Verdon, E., 2019. Dye residues in aquaculture products: targeted and metabolomics mass spectrometric approaches to track their abuse. Food Chem. 294, 355–367.
Dubreil, E., Sczubelek, L., Burkina, V., Zlabek, V., Sakalli, S., Zamaratskaia, G., Hurtaud-Pessel, D., Verdon, E., 2020b. In vitro investigations of the metabolism of Victoria pure blue BO dye to identify main metabolites for food control in fish. Chemosphere 238.
EFSA, Penninks, A., Baert, K., Levorato, S., Binaglia, M., 2017. Dyes in aquaculture and reference points for action. EFSA J. 15, e04920.
Gallart-Ayala, H., Chéreau, S., Dervilly-Pinel, G., Bizec, B.L., 2015. Potential of mass spectrometry metabolomics for chemical food safety. Bioanalysis 7, 133–146.
Gessner, T., Mayer, U., 2000. Triarylmethane and diarylmethane dyes. Ullmann's Encyclopedia of Industrial Chemistry.
Gomez, C.F., Constantine, L., Huggett, D.B., 2010. The influence of gill and liver metabolism on the predicted bioconcentration of three pharmaceuticals in fish. Chemosphere 81, 1189–1195.
Hubert, P., Nguyen-Huu, J.J., Boulanger, B., Chapuzet, E., Chiap, P., Cohen, N., Compagnon, P.A., Dewé, W., Feinberg, M., Lallier, M., Laurentie, M., Mercier, N., Muzard, G., Nivet, C., Valat, L., 2004. Harmonization of strategies for the validation of quantitative analytical procedures: a SFSTP proposal - Part I. J. Pharmaceut. Biomed. Anal. 36, 579–586.
Hubert, P., Nguyen-Huu, J.J., Boulanger, B., Chapuzet, E., Chiap, P., Cohen, N., Compagnon, P.A., Dewé, W., Feinberg, M., Lallier, M., Laurentie, M., Mercier, N., Muzard, G., Nivet, C., Valat, L., Rozet, E., 2007a. Harmonization of strategies for the validation of quantitative analytical procedures. A SFSTP proposal - Part II. J. Pharmaceut. Biomed. Anal. 45, 70–81.
Hubert, P., Nguyen-Huu, J.J., Boulanger, B., Chapuzet, E., Cohen, N., Compagnon, P.A., Dewé, W., Feinberg, M., Laurentie, M., Mercier, N., Muzard, G., Valat, L., Rozet, E., 2007b. Harmonization of strategies for the validation of quantitative analytical procedures. A SFSTP proposal-Part III. J. Pharmaceut. Biomed. Anal. 45, 82–96.
Jiang, Y., Xie, P., Liang, G., 2009. Distribution and depuration of the potentially

carcinogenic malachite green in tissues of three freshwater farmed Chinese fish with different food habits. Aquaculture 288, 1–6.
Kwan, P.P., Banerjee, S., Shariff, M., Yusoff, F.M., 2020. Persistence of malachite green and leucomalachite green in red tilapia (Oreochromis hybrid) exposed to different treatment regimens. Food Contr. 108.
Lanzing, W.J.R., 1965. Observations on malachite green in relation to its application to fish diseases. Hydrobiologia 25, 426–441.
Lewis, L.M., Indig, G.L., 2002. Effect of dye aggregation on triarylmethane-mediated photoinduced damage of hexokinase and DNA. J. Photochem. Photobiol. B Biol. 67, 139–148.
Lewis, L.M., Indig, G.L., 2001. Photonuclease activity of mitochondrial triarylmethane photosensitizers. Pharmaceut. Pharmacol. Lett. 11, 22–25.
Máchová, J., Svobodová, Z., Svobodník, J., Piačka, V., Vykusová, B., Kocová, A., 1996. Persistence of malachite green in tissues of rainbow trout after a long-term therapeutic bath. Acta Vet. 65, 151–159.
Ngan, D.K., Ye, L., Wu, L., Xia, M., Rossoshek, A., Simeonov, A., Huang, R., 2019. Bioactivity signatures of drugs vs. Environmental chemicals revealed by Tox21 high-throughput screening assays. Front. Big Data 2.
Okocha, R.C., Olatoye, I.O., Adedeji, O.B., 2018. Food safety impacts of antimicrobial use and their residues in aquaculture. Publ. Health Rev. 39.
Plakas, S.M., El Said, K.R., Stehly, G.R., Gingerich, W.H., Allen, J.L., 1996. Uptake, tissue distribution, and metabolism of malachite green in the channel catfish [Ictalurus punctatus]. Can. J. Fish. Aquat. Sci. 53, 1427–1433.
Poe, W.E., Wilson, R.P., 1983. Absorption of malachite green by channel catfish. Prog. Fish-Cult. 45, 228–229.
RASFF-portal. European Commission. https://webgate.ec.europa.eu/rasff-window/portal/.
Schnick, R.A., 1988. The impetus to register new therapeutants for aquaculture. Prog. Fish-Cult. 50, 190–196.
Schultz, I.R., Hayton, W.L., 1999. Interspecies scaling of the bioaccumulation of lipophilic xenobiotics in fish: an example using trifluralin. Environ. Toxicol. Chem. 18, 1440–1449.
Srivastava, S., Sinha, R., Roy, D., 2004. Toxicological effects of malachite green. Aquat. Toxicol. 66, 319–329.
Sudova, E., Machova, J., Svobodova, Z., Vesely, T., 2007. Negative effects of malachite green and possibilities of its replacement in the treatment of fish eggs and fish: a review. Vet. Med. 52, 527–539.
Tacal, O., Özer, I., 2007. An assessment of the role of intracellular reductive capacity in the biological clearance of triarylmethane dyes. J. Hazard Mater. 149, 518–522.
Verdon, E., Bessiral, M., Chotard, M.P., Couëdor, P., Fourmond, M.P., Fuselier, R., Gaugain, M., Gautier, S., Hurtaud-Pessel, D., Laurentie, M., Pirotais, Y., Roudaut, B., Sanders, P., 2015. The monitoring of triphenylmethane dyes in aquaculture products through the European Union network of official control laboratories. J. AOAC Int. 98, 649–657.